Rational design of materials with tailored functionalities

A. K. Tyagi

Chemistry Division
Bhabha Atomic Research Centre
Mumbai

Email: aktyagi@barc.gov.in

Materials of today and tomorrow

Indian Academy of Sciences Meeting, BHU, Varanasi (2-11-2018)

Design of new functional materials

Crystallographic approach

Metastable materials

Defects

Hybrid materials

Preparation methods

Ceramic method	**Solid State Synthesis**
Soft-chemical methods	**Combustion synthesis, template method, polyol method, sono-chemical, miceller methods, impregnation, hydro & solvothermal methods, xero-gel method, solid state metathesis**
Other methods	**Intercalation / Deintercalation** **High pressure synthesis** **Vacuum heat treatment** **Melt and quench technique**
Processing	**Ink-jet printing, screen printing and spin coating**

Design of materials with tailored magnetic properties and band gap

Novel synthesis of Ce^{3+} based oxides

Challenge: To develop a facile route for Ce(III) stabilization

Two steps synthesis:

(i) Combustion method
(ii) Vacuum heating in reducing atmosphere

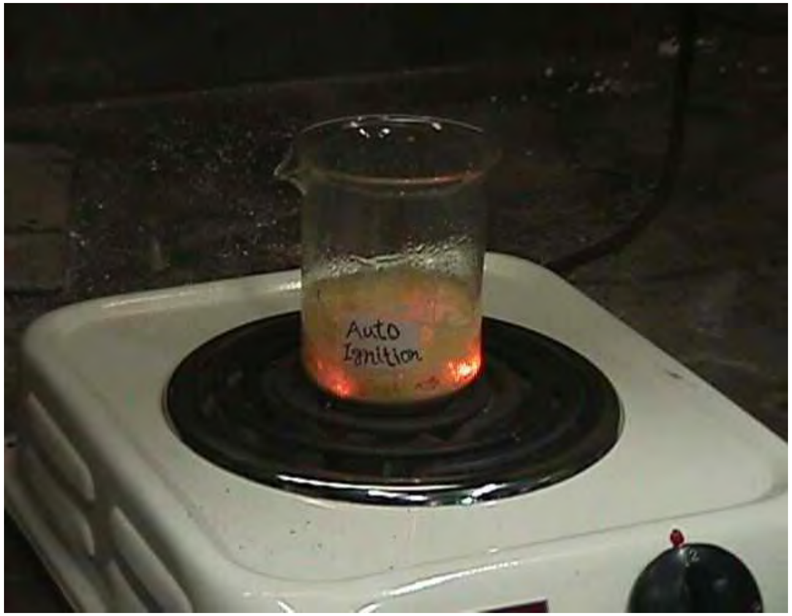

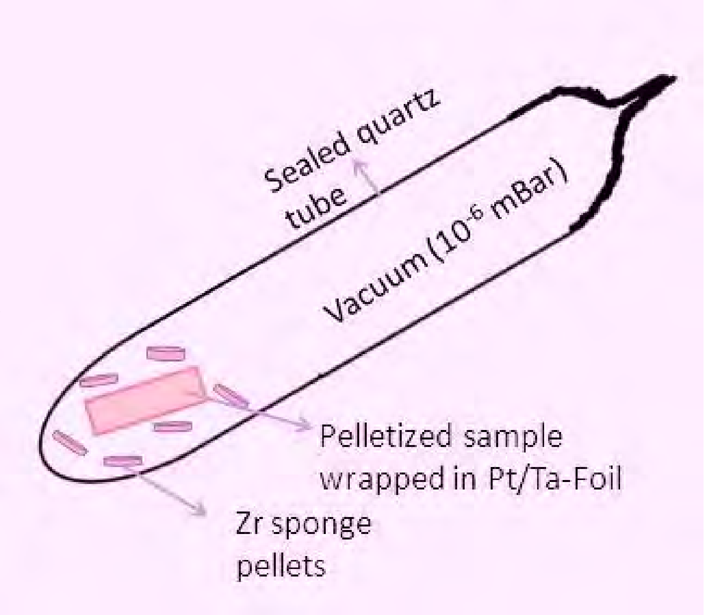

$CeCrO_3$: A multi-functional material

Band Gap : 3.04eV, Crystallite size: 42 nm

TEM

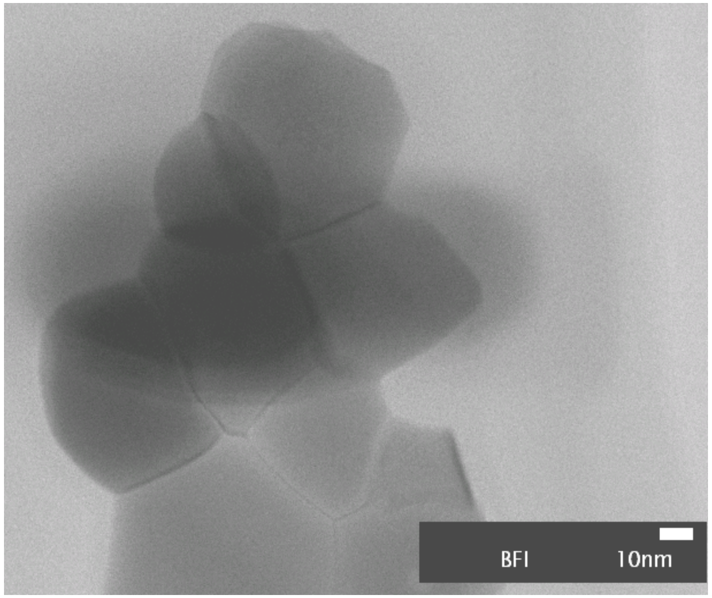

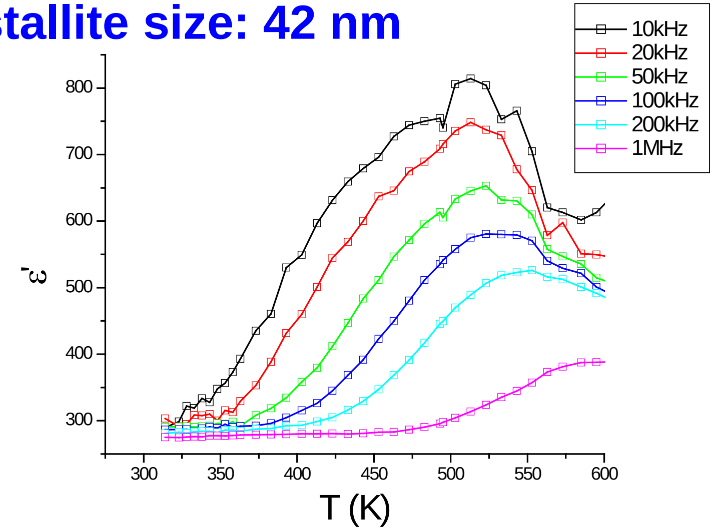

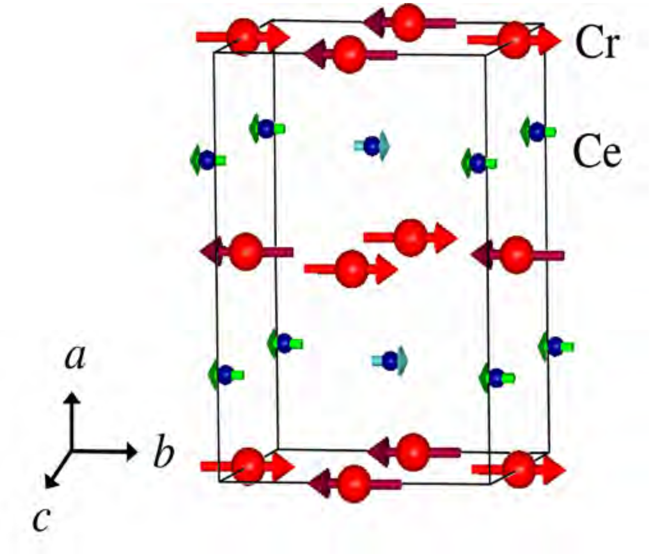

- **Relaxor ferroelectricity**
- **Antiferromagnetism**
- **Photocatalysis**

J. Phys. Chem. C 113 (2009) 12663

Magnetic studies: Dr. S. M. Yusuf

$La_{1-x}Ce_xCrO_3$ $(0.0 \leq x \leq 1.0)$: A new series of solid solutions with tunable magnetic and optical properties

By a conventional solid state method only about 20 mol % of Ce^{3+} can be incorporated in $LaCrO_3$ lattice

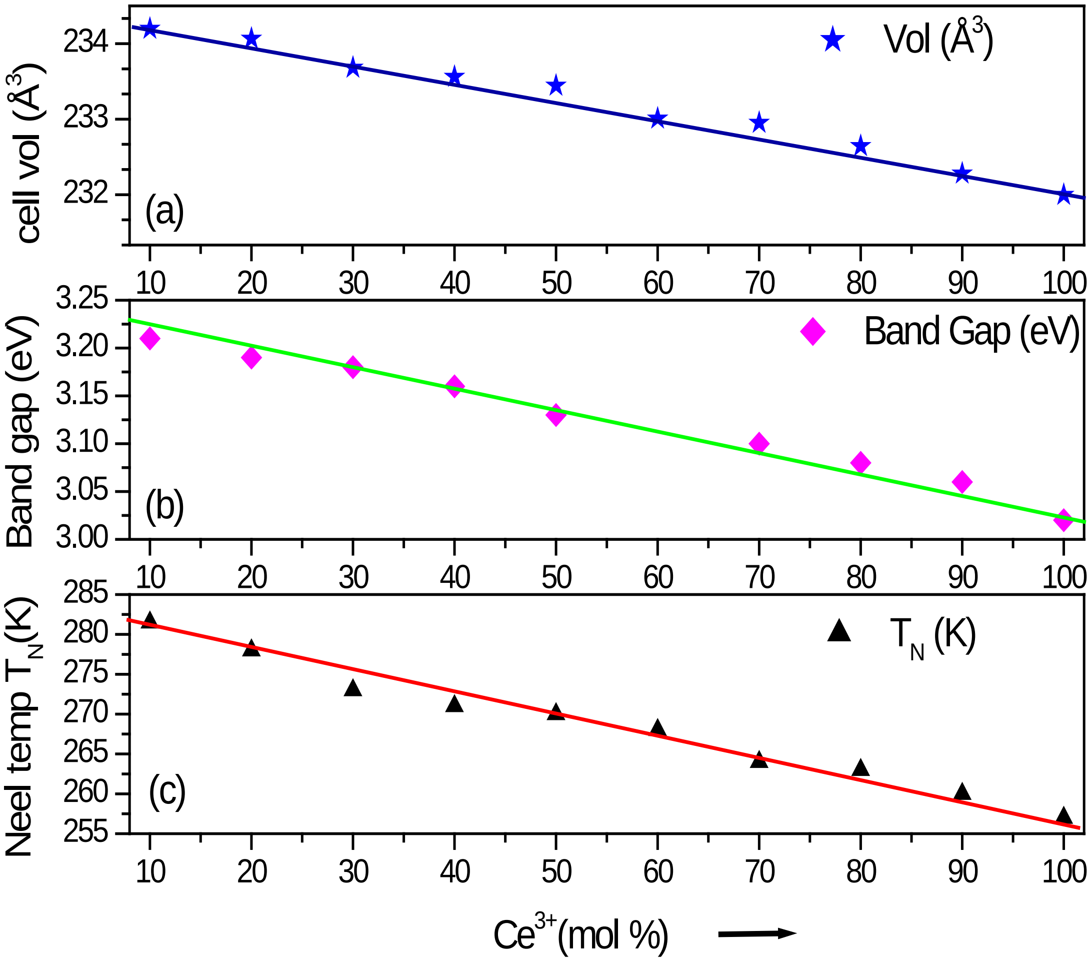

Ideal solid solution formation (Orthorhombic: Sp. Gr: Pbnm)

Tunable band gap from 3.21eV to 3.04 eV

Linear trend of T_N from 282 K to 257 K

Magnetization data for $La_{1-x}Ce_xCrO_3$ series

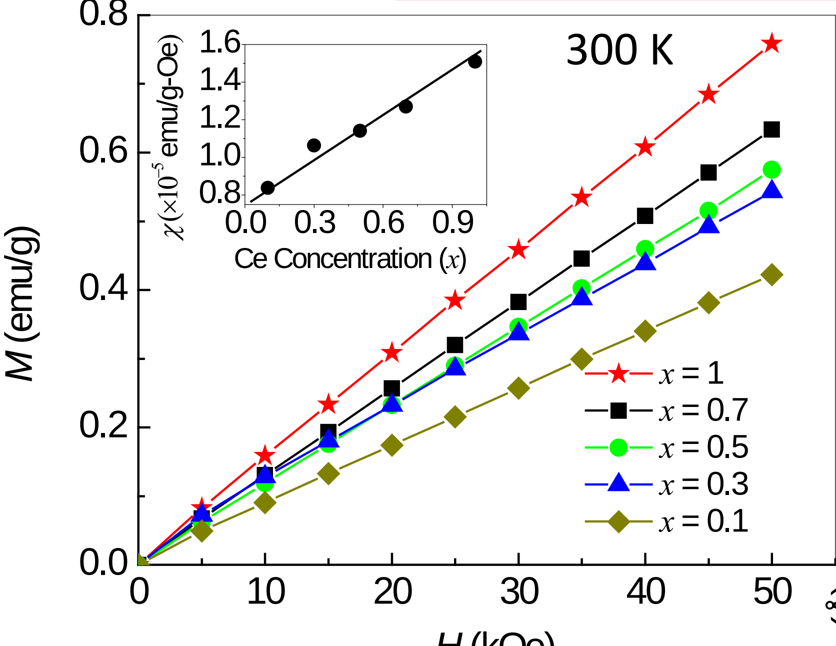

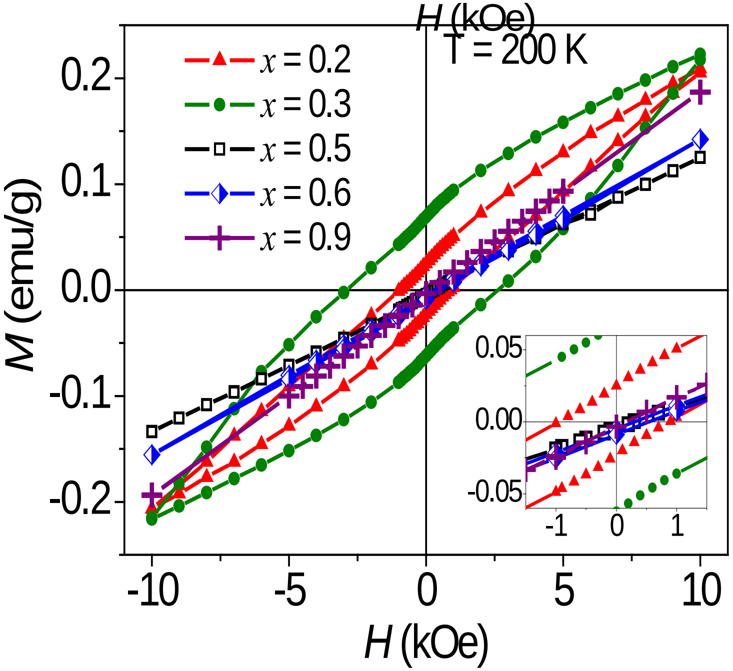

Distortion Parameter calculation

$$\Delta = \left(\tfrac{1}{6}\right)\sum_{i=1}^{6}\{(d_i - \langle d \rangle)/\langle d \rangle\}^2$$

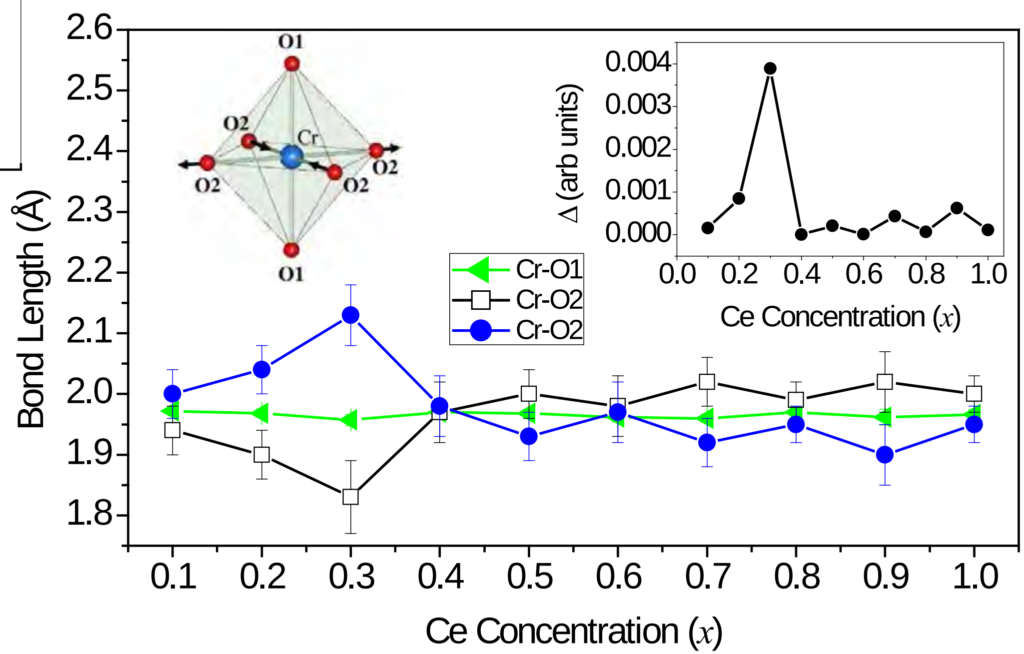

Inorganic Chemistry 48 (2009) 11691

A new series of solid solution in $Pr_{1-x}Ce_xScO_3$ ($0.0 \leq x \leq 1.0$)

Close ionic radii of Pr^{3+} (1.12 Å) & Ce^{3+} (1.14 Å)

No reason to hinder the formation of $Pr_{1-x}Ce_xScO_3$ series

Gel-combustion followed by reduction

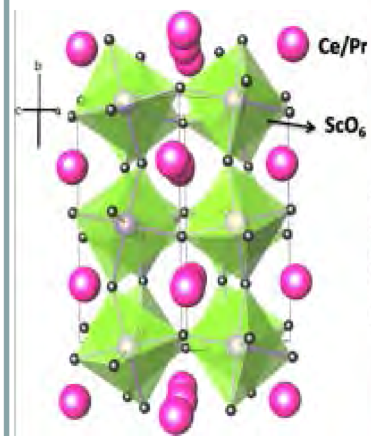

Perovskite Structure

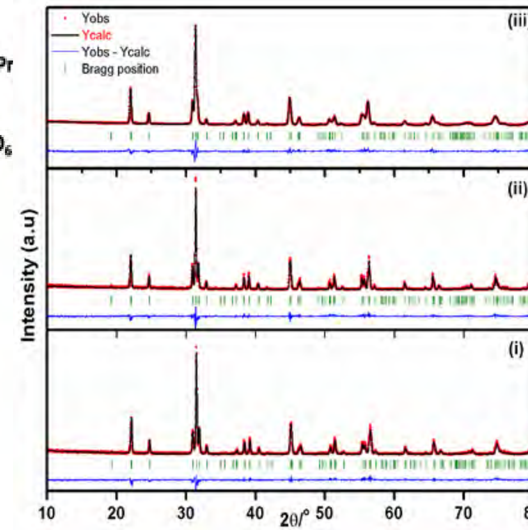

Rietveld fitted pattern

Bandgap tunability : 4.74 - 2.91 eV

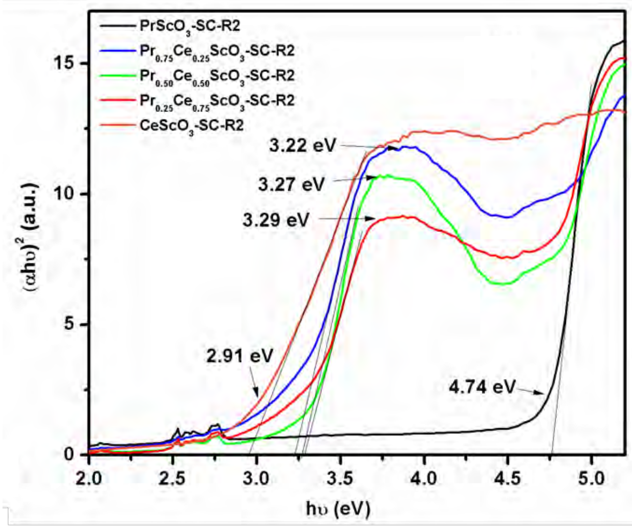

Photocatalytic degradation of Rh

$t_{1/2}$ = 300 min

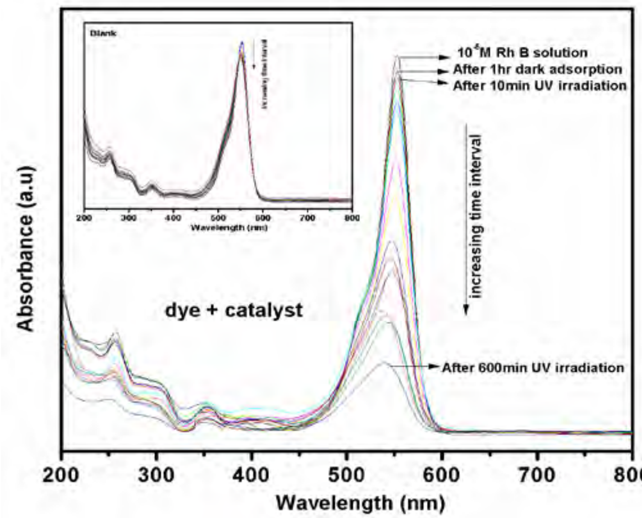

Dalton Trans. 44 (2015) 16929

Design of oxygen storage materials

Preparation of $CeScO_3$: A multi-functional material

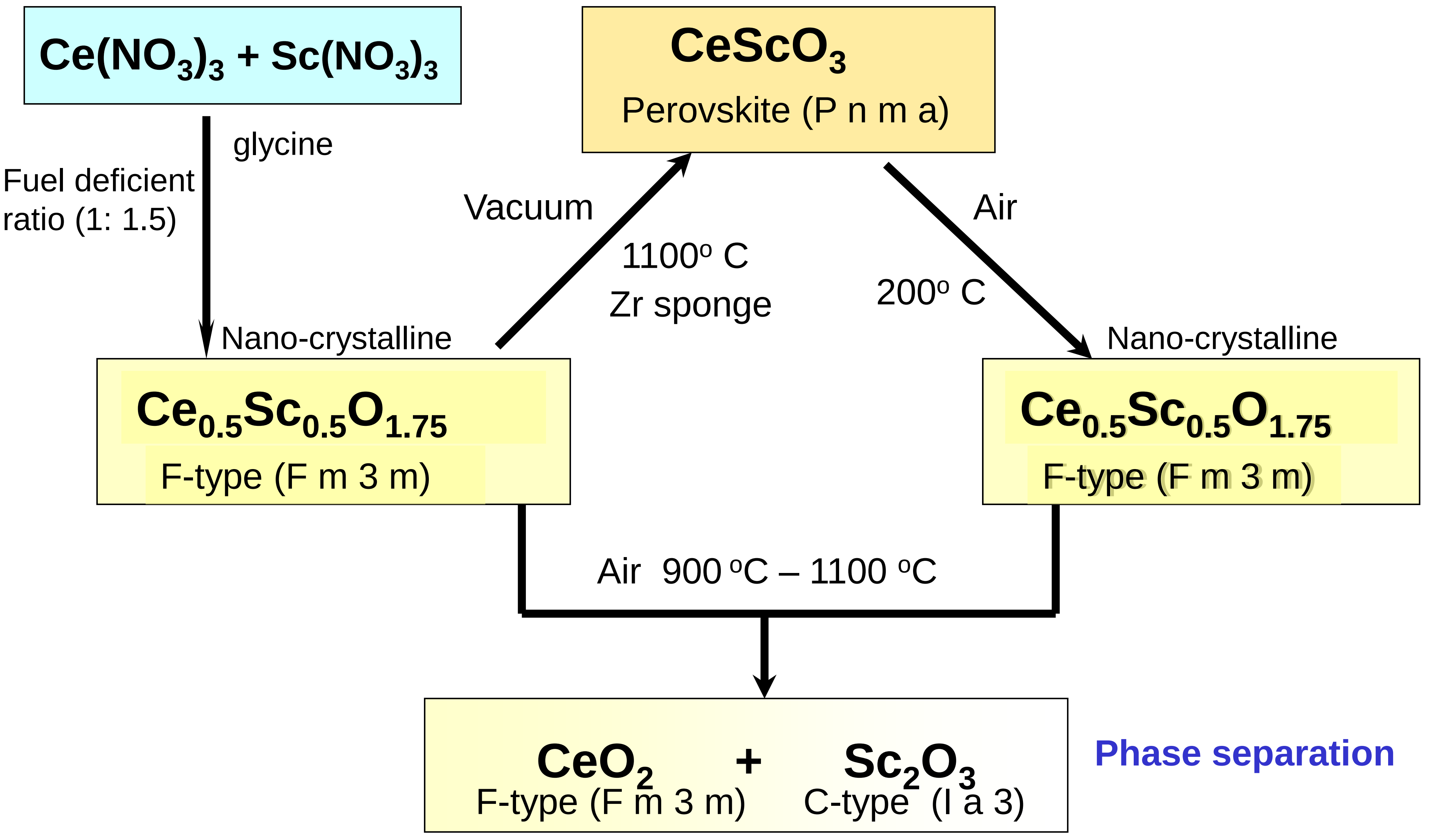

CeO_2 and Sc_2O_3: Limited solubility by solid state route

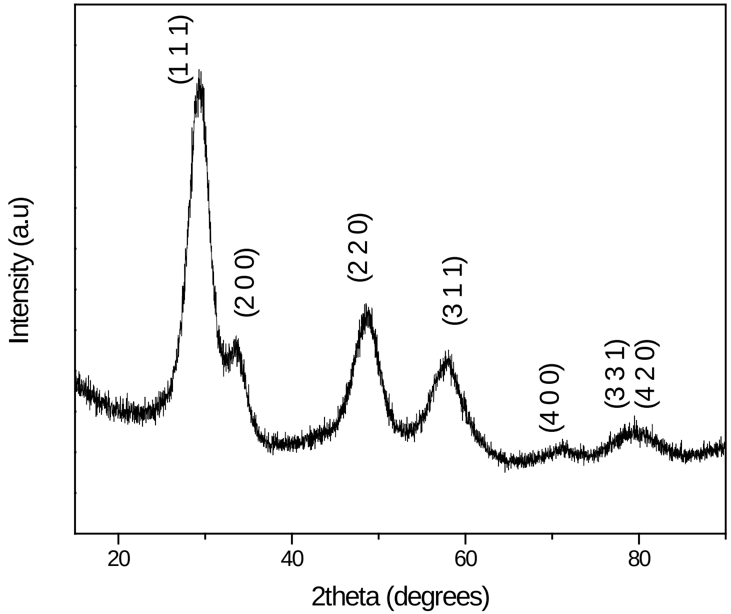

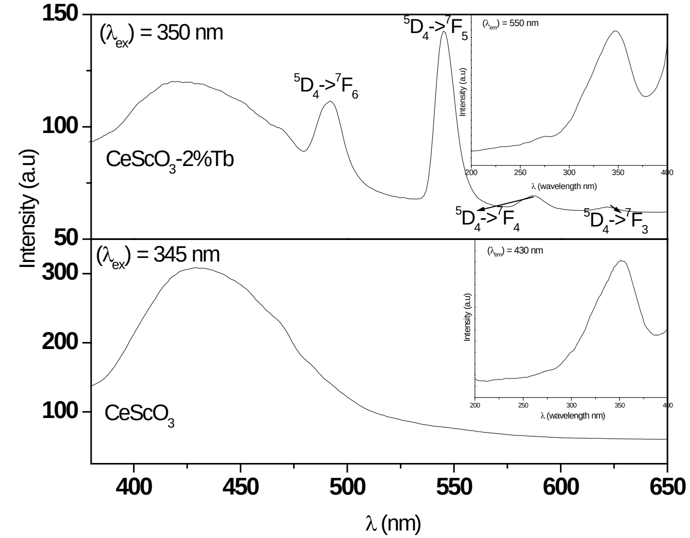

XRD of $Ce_{0.5}Sc_{0.5}O_{1.75}$

PL spectra of $CeScO_3$ and 2% Tb^{3+} doped $CeScO_3$

- **Magnetization revealed $CeScO_3$ to be paramagnetic**
- **$CeScO_3$ was found to have band gap of 3.2 eV**
  (Low band gap is due to mixing of O p, Sc d and Ce d states)
- **$CeScO_3$ is a potential host material giving broad blue emission.**

Inter-conversion between a perovskite and fluorite lattice

$Ce_{0.5}Sc_{0.5}O_{1.75}$ (Fluorite)

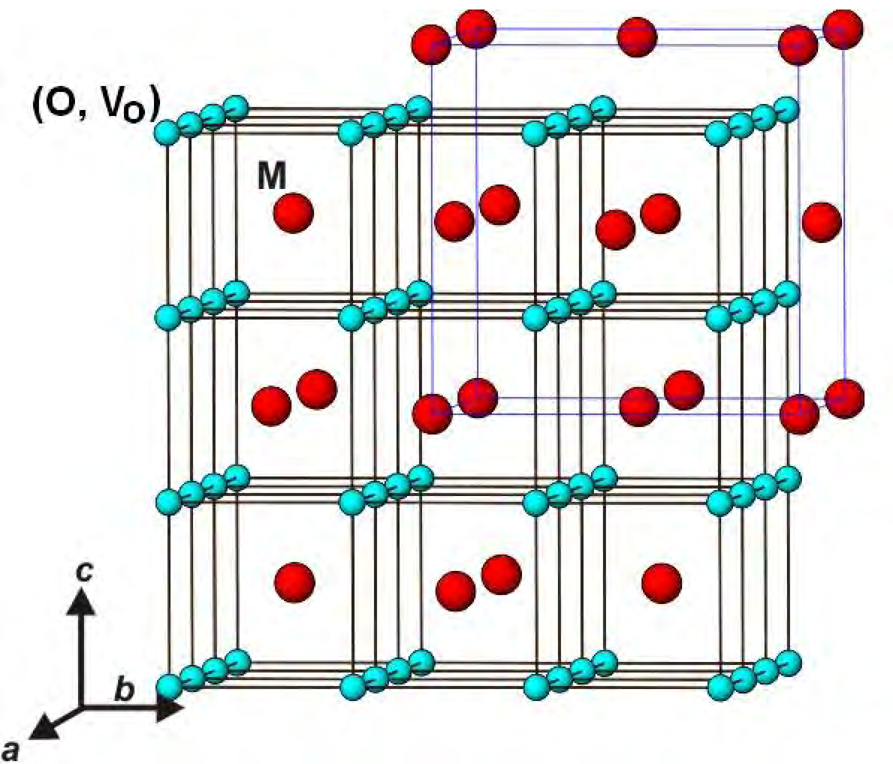

reduction

oxidation

$CeScO_3$ (Perovskite)

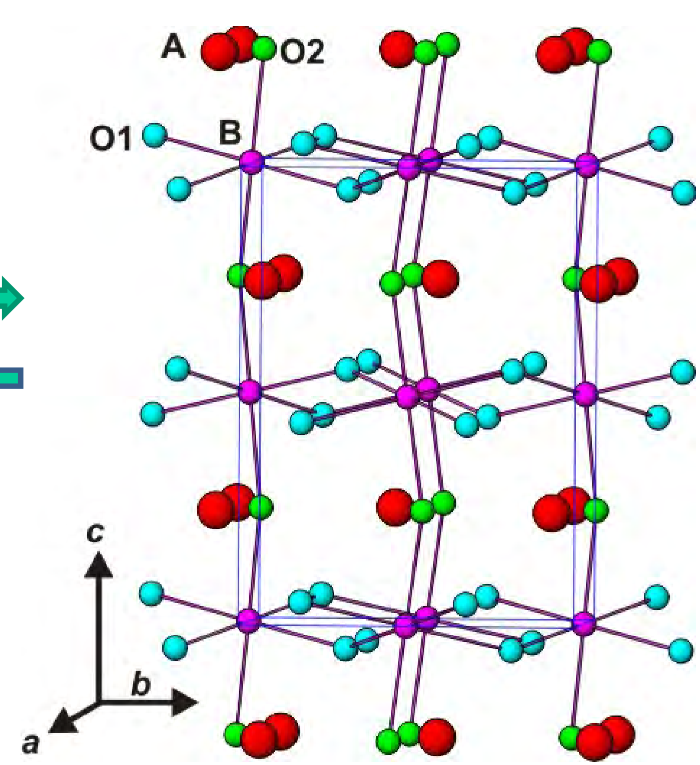

F m 3 m; a = 5.3409 (12) Å

P n m a
a = 5.7772 (1) Å ,
b = 8.0473 (1) Å
c = 5.6429 (1) Å

$CeCrO_3$ does not show this inter-conversion

Inorganic Chemistry, 49 (2010) 1152

Ce-Zr-O system ($Ce_2Zr_2O_{7+x}$): Oxygen storage capacitor

a = 10.6924(3) Å
ρ = 6.245 g/cc

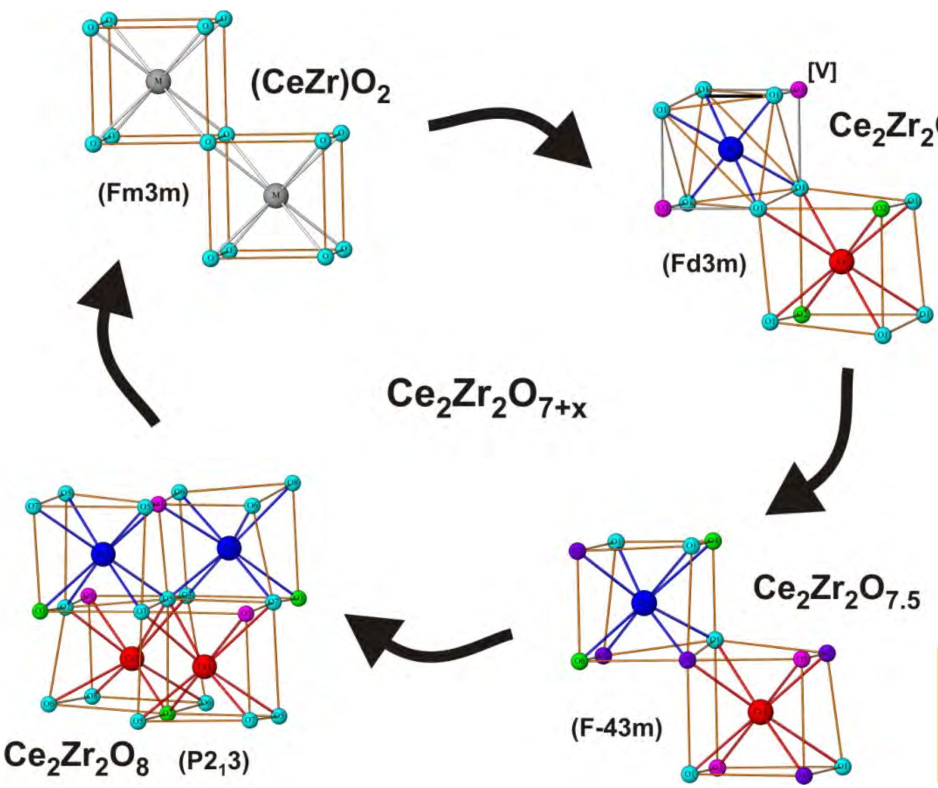

a = 10.6199(2) Å
ρ = 6.466 g/cc

a = 10.5433(2) Å
ρ = 6.693 g/cc

$Ce_2Ti_2O_7$ pyrochlore does not show OSC

Applications: Redox catalysis

Chemistry of Materials 29 (2009) 5848

Oxidative dehydrogenation of ethyl benzene to yield styrene using Ce-Zr-O Catalyst

A technologically important reaction

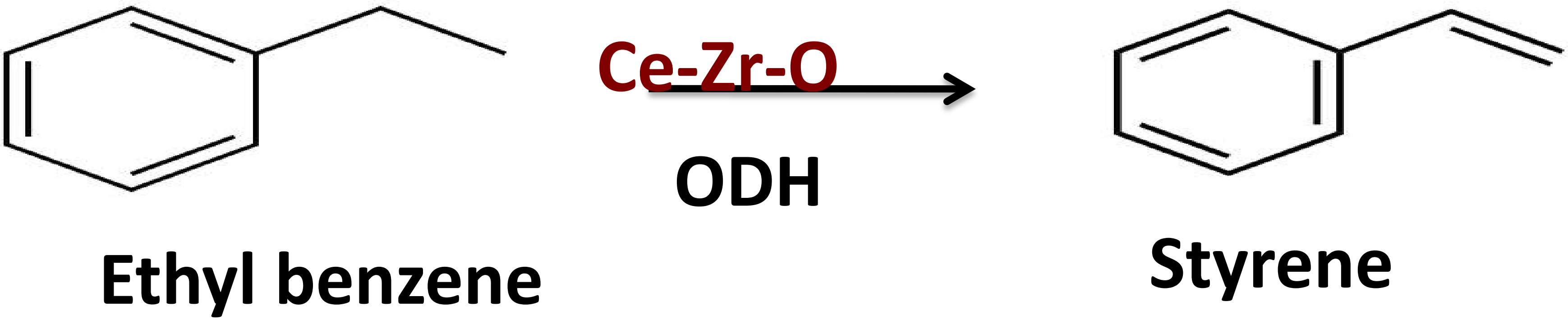

Salient features of the reaction

- No degradation of catalyst (72 h)
- 93-95% selectivity achieved in temperature range of 450 -550^{o}C
- Yield approximate 50 % at 550^{o} C
- Highly reproducible

Collaborator: Dr. T. Raja, NCL Pune

Oxidative dehydrogenation of ethyl benzene to yield styrene

Characterization

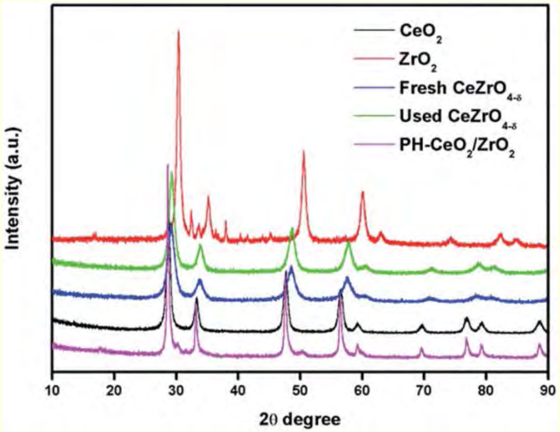

XRD

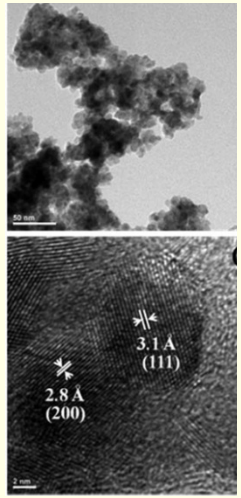

TEM
Fresh catalyst

Characterization

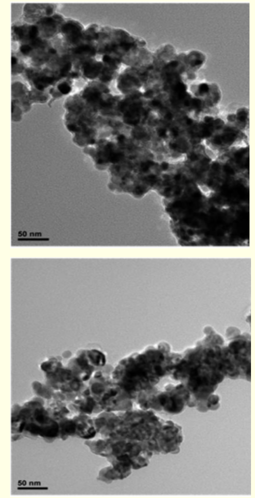

TEM
used catalyst

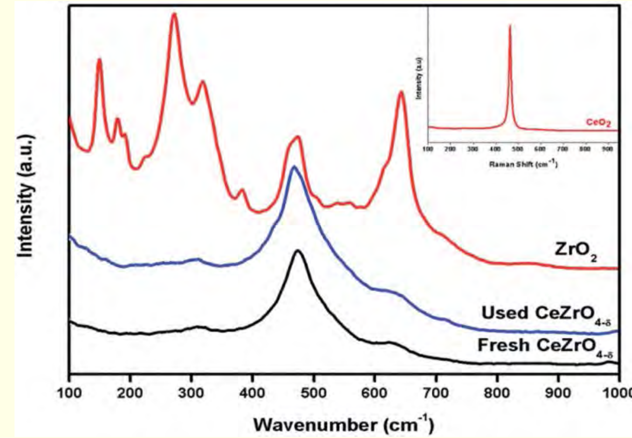

Raman

Catalytic activity at 550 °C

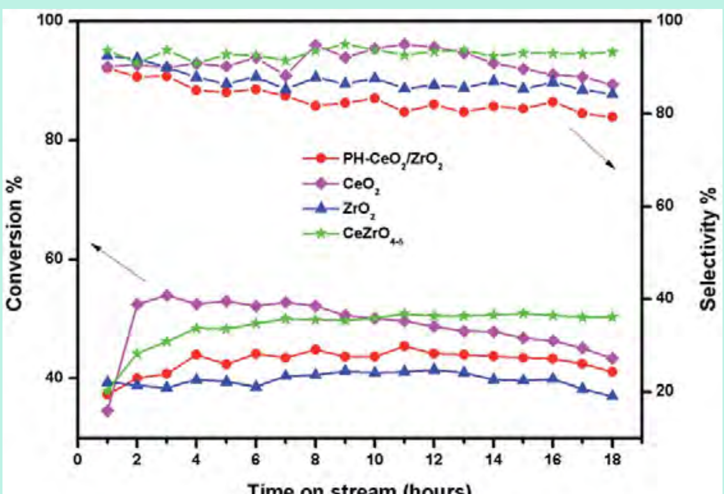

Conversion and selectivity

No degradation of catalyst (72 h)

Highly reproducible

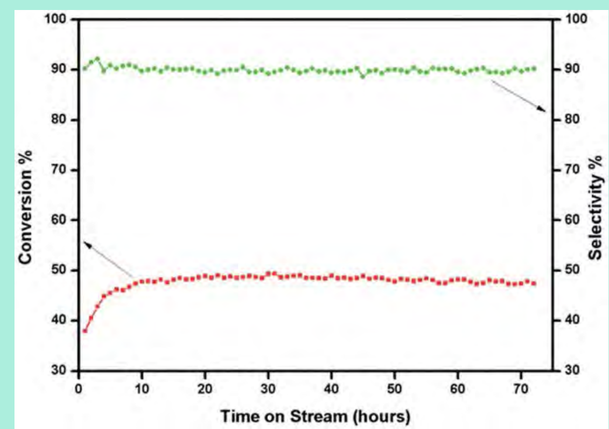

RSC Advances 5 (2015) 3619

Palladium supported Ce-Zr-O for heterogeneous Suzuki coupling in water :A green protocol

Model Suzuki reaction:

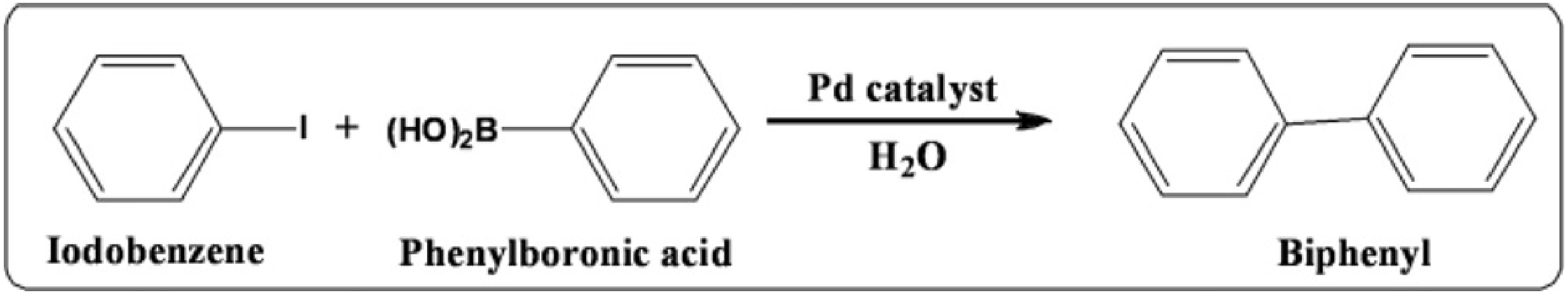

Aryl halide	% Conversion
C_6H_5Cl	42
C_6H_5Br	97
C_6H_5I	100

ICP-AES: No leaching of Pd into the solution (below 1 ppm)

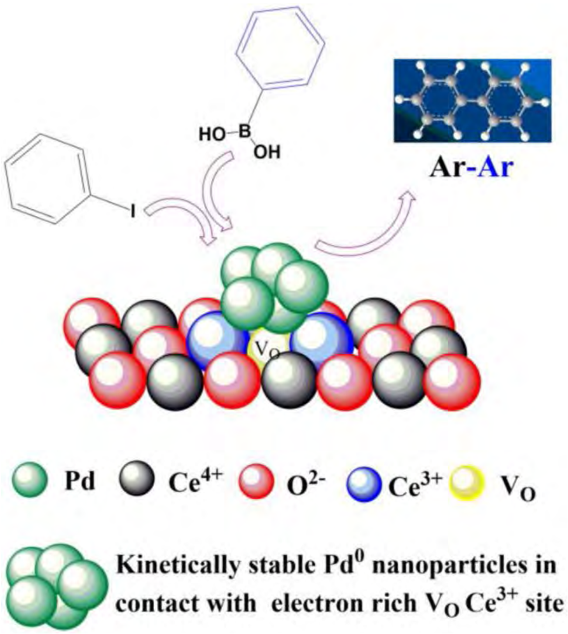

Efficient protocol for Suzuki cross coupling reaction over new support Ce-Zr-O

Use of green solvent water

Significant activity for less reactive aryl bromides.

Role of reducible support Ce-Zr-O on catalytic activity

Presence of slight Ce^{3+} on support enhances the activity

Chemistry Select 1 (2016) 2673

Suzuki cross coupling with various aryl halides & aryl boronic acids

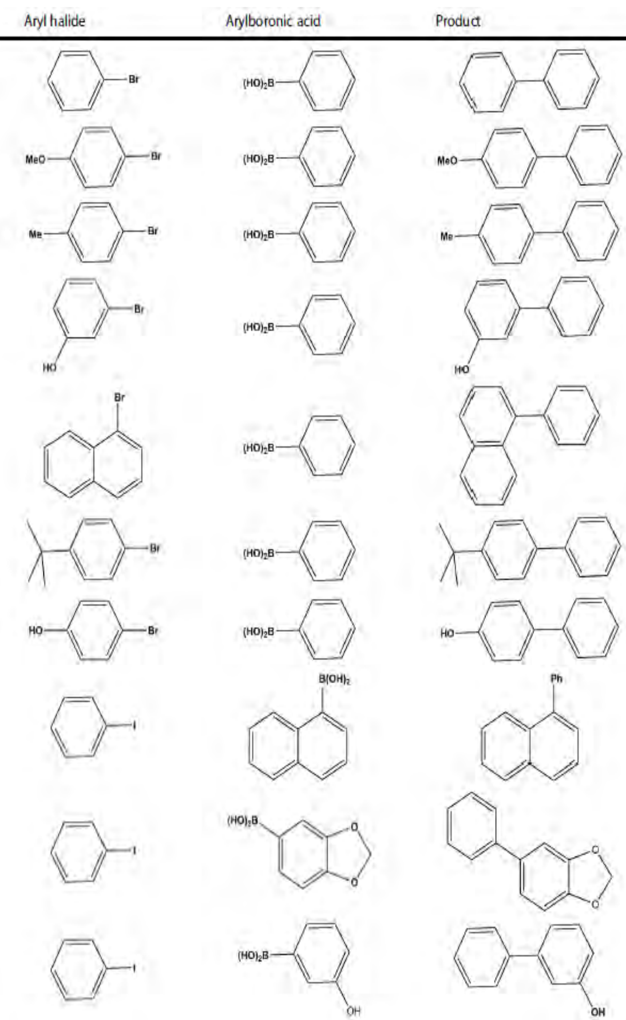

Entry	Time (h)	Yield (%)[b]
1	1.3	98
2	4	99
3	3.5	96[c]
4	6	95
5	5	79
6	8	84
7	4	83
8	6	76
9	10	60
10	6	72

Collaborator: Dr. Gopinath, NCL Pune

CO oxidation: $CeZrO_{4-\delta}$ supported Pd catalysts

$CeZrO_{4-\delta}$ was prepared by gel-combustion method
Palladium (1 wt% loading) by photo-deposition technique

50 mL/min flow rate (CO: O_2: N_2 = 1:5:19)

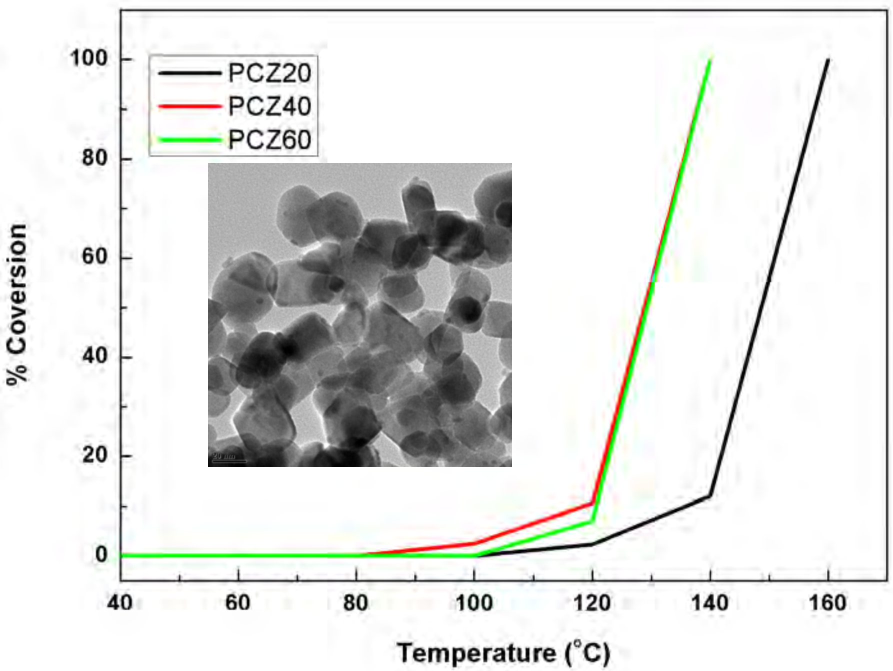

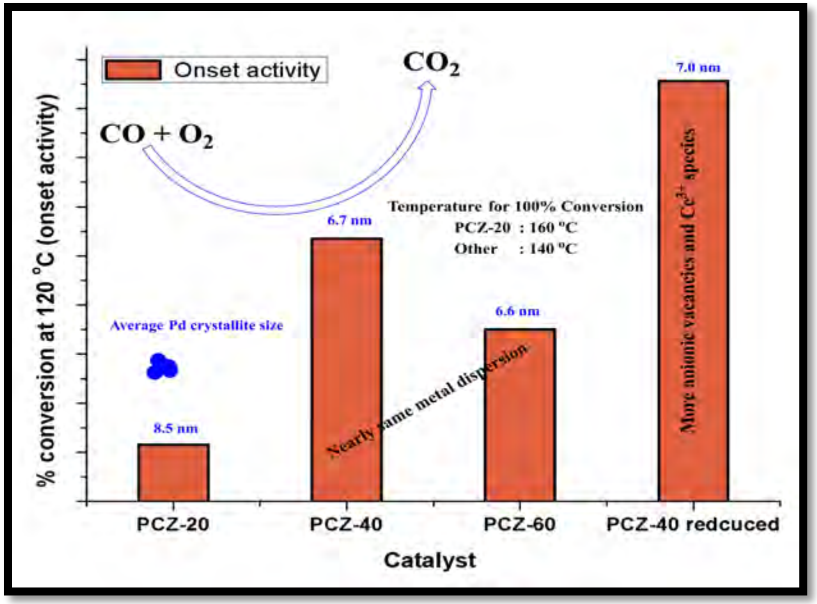

100% conversion was achieved at 140 ^{0}C with sustainability of the catalyst for 12 h.

Molecular Catalysis 455 (2018) 1

Design of ionic conductors

Ionic Conductivity...

$$\sigma_{dc} = \sigma_0 \exp(-E / k_B T)$$

σ_{dc} = dc conductivity
E = Activation Energy
k_B = Boltzmann Constant
T = Temperature

σ_{dc} can be increased by

either

Increasing σ_o (increasing mobile species)

or

Decreasing E (improving degree of order)

or

Manipulating both

Raman Spectra of $Nd_{2-y}Gd_yZr_2O_7$

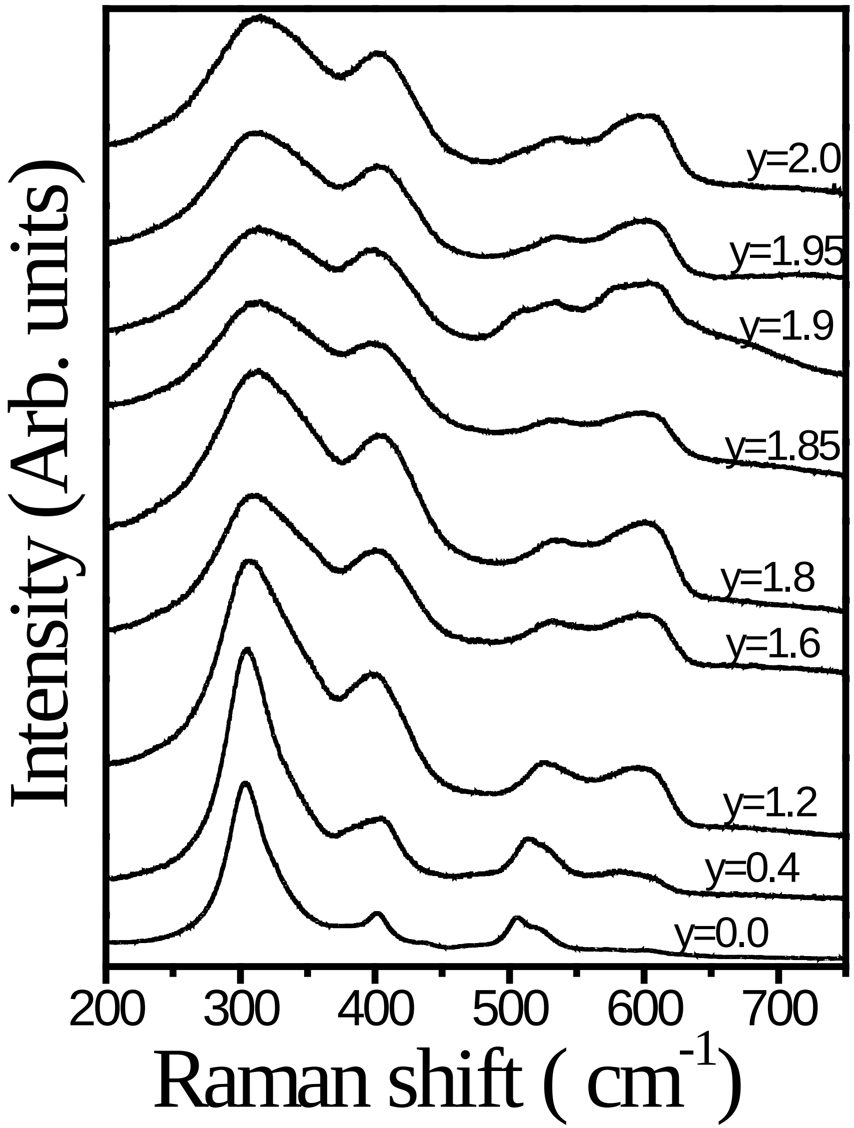

$Gd_2Zr_2O_7$

Disorder increases

$Nd_2Zr_2O_7$

Corroborated by XRD also

On moving from $Gd_2Zr_2O_7$ to $Nd_2Zr_2O_7$

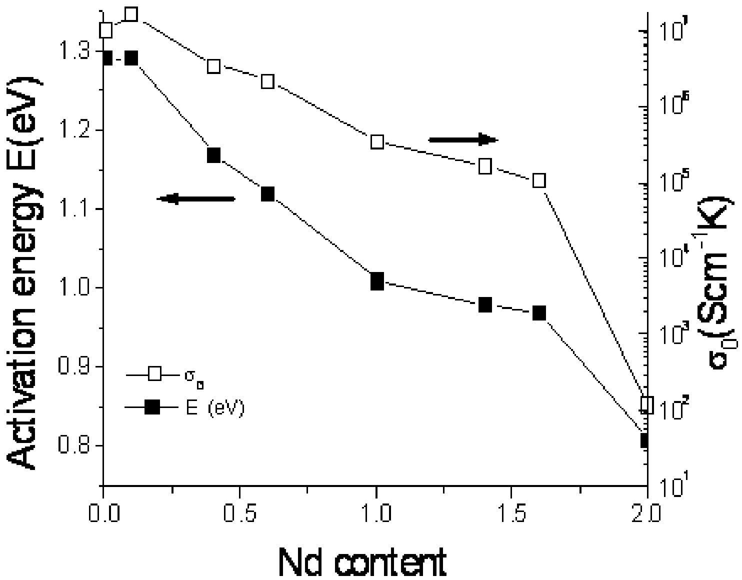

Decrease in activation energy

Improve ionic conductivity

Decrease of no. of mobile species

Reduces the conductivity

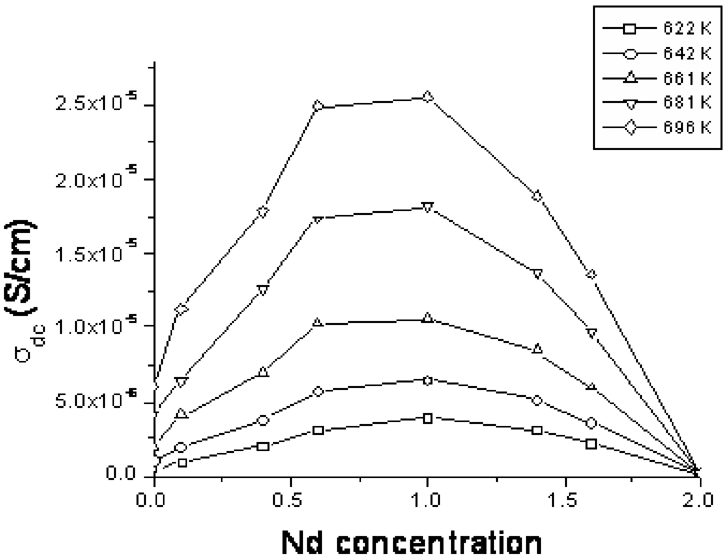

Conductivity is maximum for y ≈ 1.0 in $Nd_{2-y}Gd_yZr_2O_7$

J. Mater. Res. 23 (2008) 911

Improved ionic conductivity in $NdGdZr_2O_7$: Influence of Sc^{3+} substitution

- Effect on ionic conductivity by aliovalent substitution (Replacing Zr^{4+} with Sc^{3+})
- Synthesis by gel combustion method

XRD

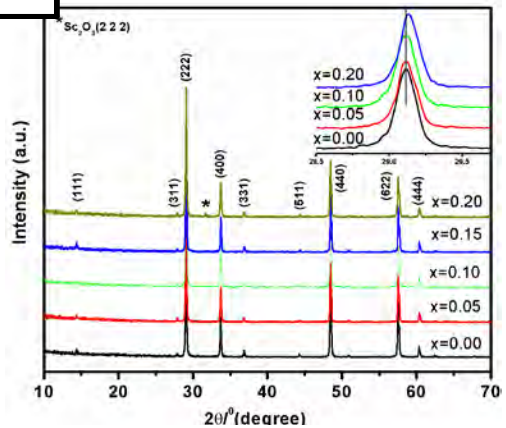

Solubility till x=0.15

Raman

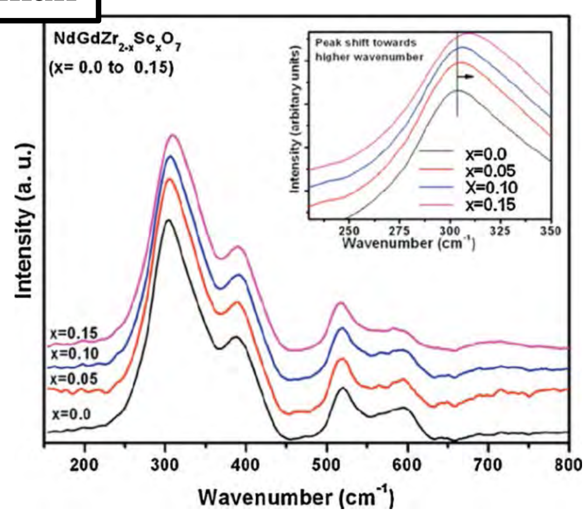

From impedance spectroscopy

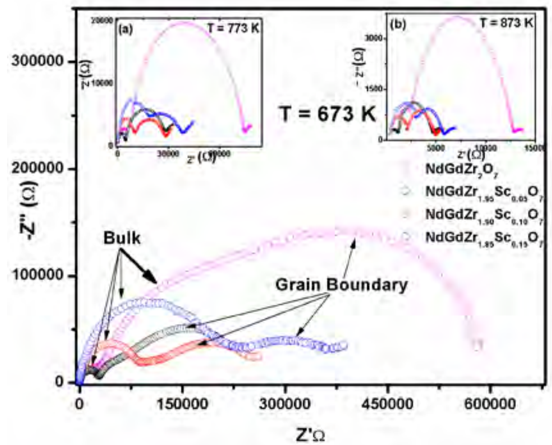

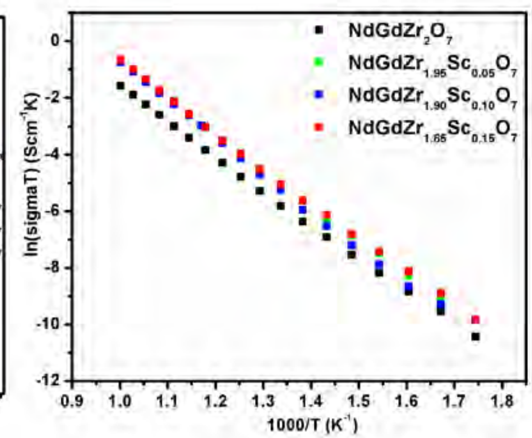

Sample composition	Activation energy E_a(eV)	Pre-exponential factor A (S cm^{-1} K)	923K (S-cm^{-1})
X=0.00	1.011	2.26 x 10^4	7.97 x10^{-5}
X=0.05	1.052	9.34 x 10^4	1.89 x10^{-4}
X=0.10	1.061	10.23 x 10^4	1.88 1x10^{-4}
X=0.15	1.126	21.70 x 10^4	1.73 x10^{-4}

J. Eur. Ceram. Soc. 32 (2012) 3221

Structural control of ionic conductivity without hetero-ion: $Nd_{2-x}Zr_{2+x}O_{7+x/2}$ ($-0.2 \leq x \leq 0.4$)

XRD Patterns

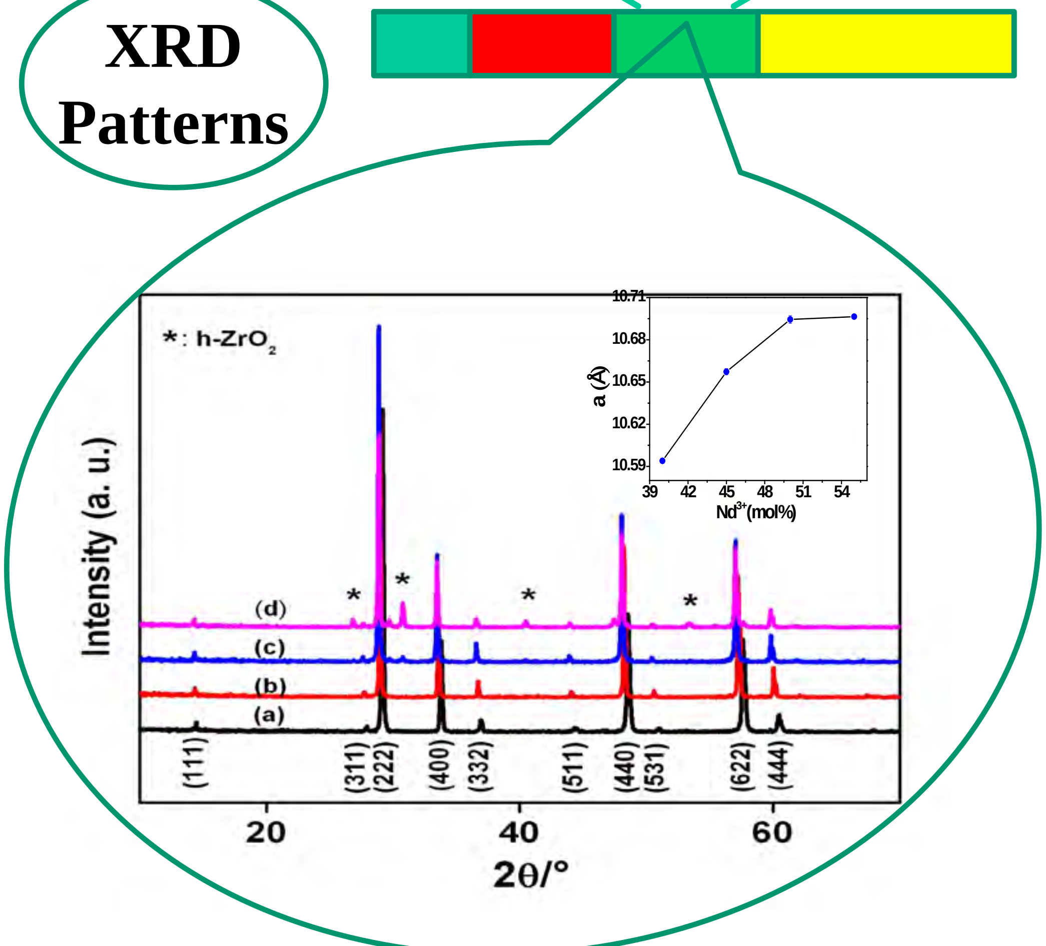

Raman spectra

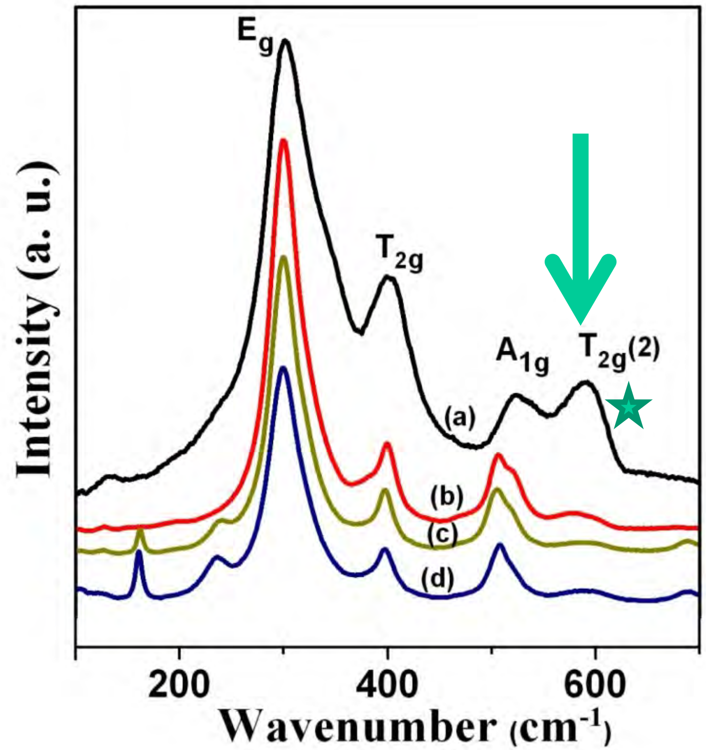

All pyrochlores phase field

Difference in local structures

✓ From (a) to (d) Nd content increases from 40 mol% to 55 mol%

Arrhenius Plots for dc conductivity

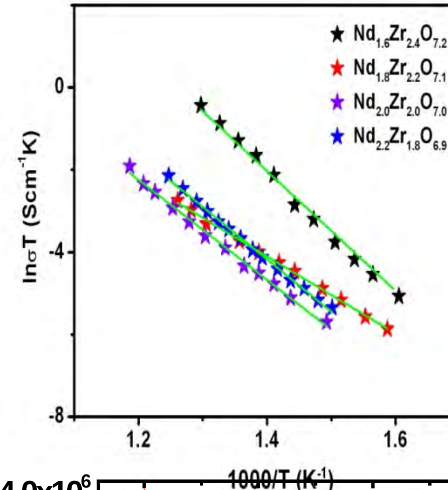

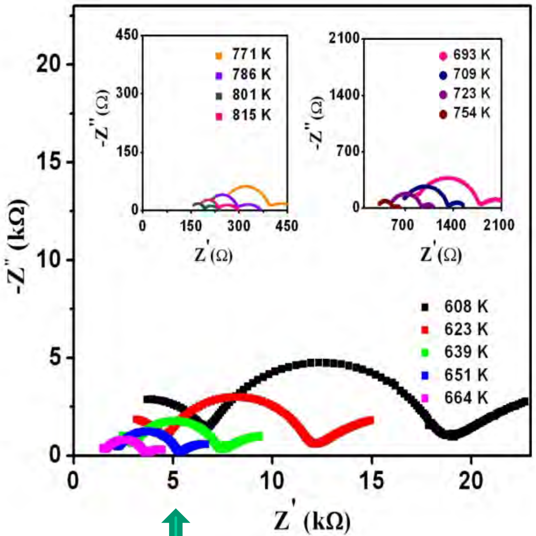

Variation of properties with Nd^{3+} content

Representative Nyquist Plots

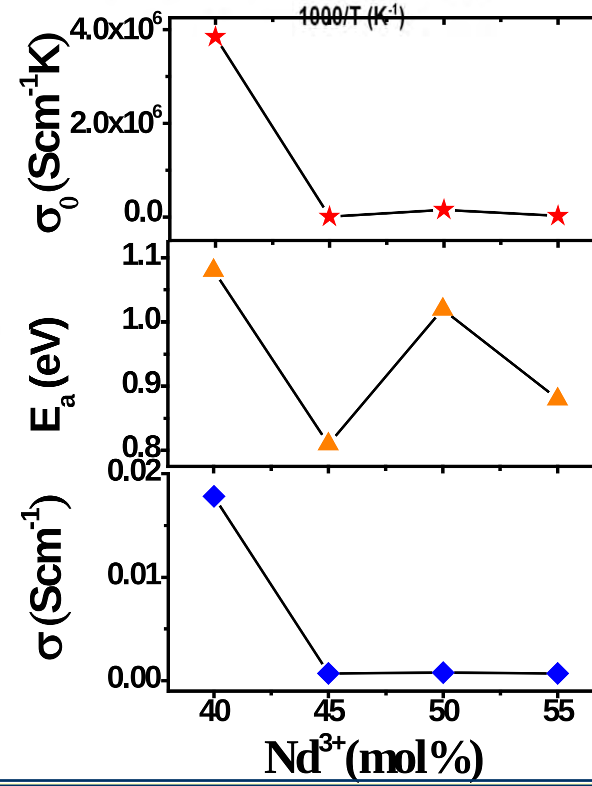

Composition	E_a (eV)	σ_0	σ [Scm^{-1}] (at 973 K)
$Nd_{1.6}Zr_{2.4}O_{7.2}$	*1.08(2)*	*3.84×10^6*	*0.018*
$Nd_{1.8}Zr_{2.2}O_{7.1}$	*0.81(1)*	*8.27×10^3*	7.17×10^{-4}
$Nd_{2.0}Zr_{2.0}O_{7.0}$	1.02(2)	1.53×10^5	7.69×10^{-4}
$Nd_{2.2}Zr_{1.8}O_{6.9}$	0.88(1)	2.55×10^4	7.22×10^{-4}

RSC Advances 6 (2016) 97566

Design of materials with tailored dielectric properties

$GdSc_{1-x}In_xO_3$ ($0.0 \leq x \leq 1.0$) system

(Materials with tunable electrical properties)

- **Altering B-site co-ordination: Changes in structure and implications on electrical properties**

B-site CN: 6 (Orthorhombic sp.gr.: *Pnma*; Centrosymmetric dielectric

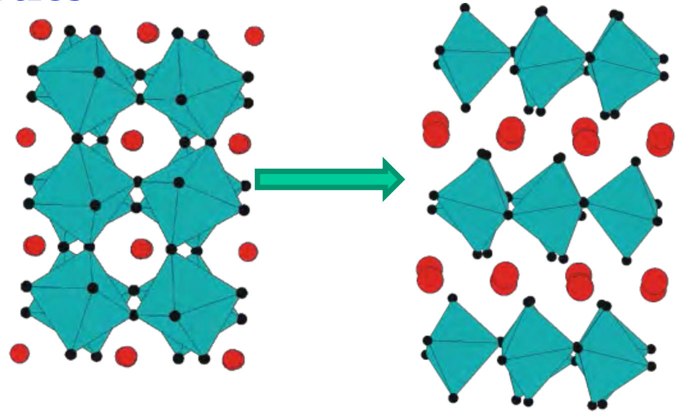

GdScO$_3$ **GdInO$_3$**

B-site CN: 5;Hexagonal; Sp.gr.: $P6_3cm$; Non-centrosymmetric; Proposed ferroelectric

Synthesis: Conventional solid state; glycine-aided gel combustion (GC)

- **GC: Increase in solubility of In^{3+} by 20 mol% !!!**

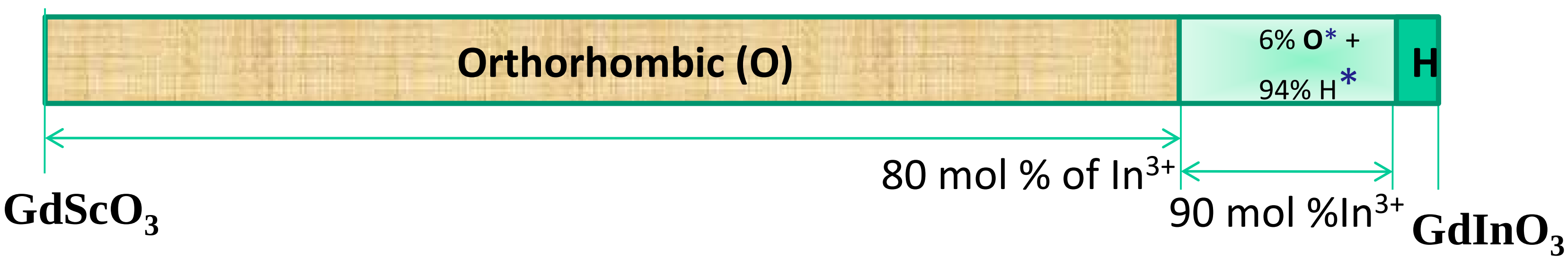

Raman Spectroscopy

- supports XRD results
- Interesting: No variation in modes due to A vibrations in orthorhombic phase field => Abrupt Structural change.

XRD

- Single-phasic orthorhombic till 80 mol% In^{3+} => Stability of In^{3+} in both 6-fold and 5-fold co-ordination
- Lattice parameters increase with increase in In^{3+} content

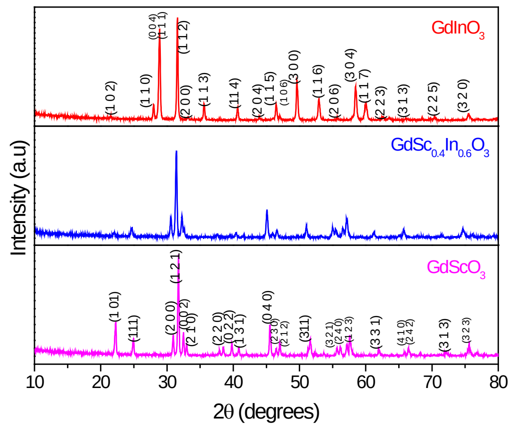

Characterisations

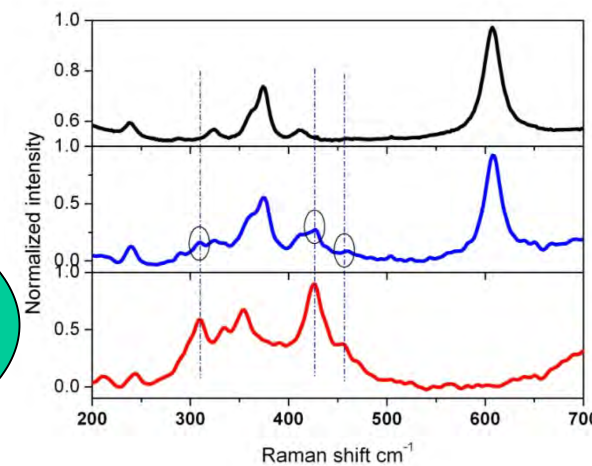

Thermo-mechanical analysis

- Net shrinkage follows the same trend as theoretical densities calculated.

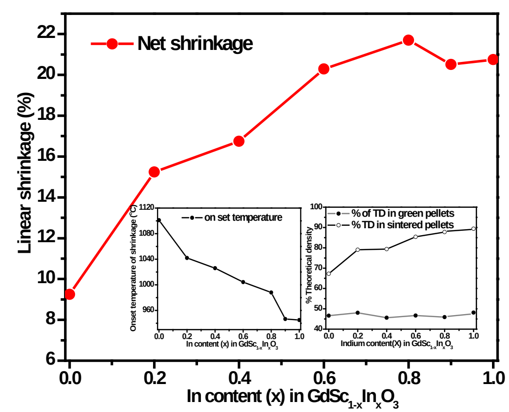

Tunability of electrical behavior

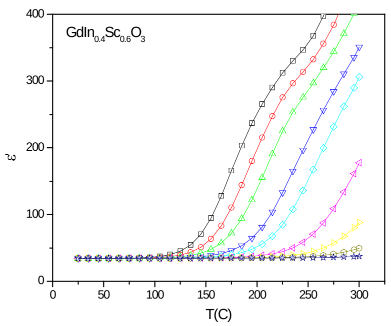

80 mol% In^{3+}

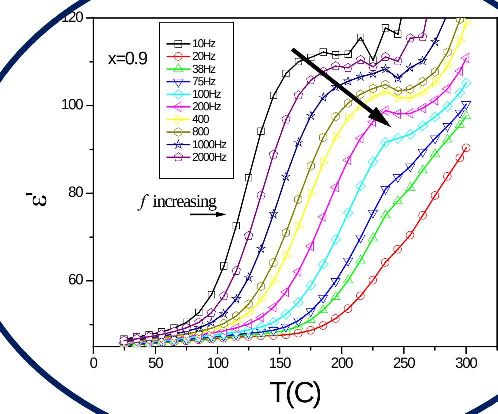

90 mol% In^{3+}

100 mol% In^{3+}

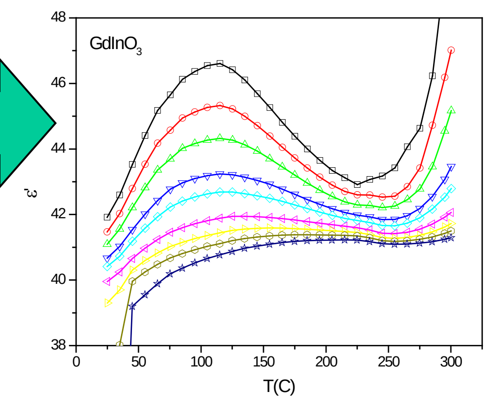

Classical relaxor ferroelectric behavior

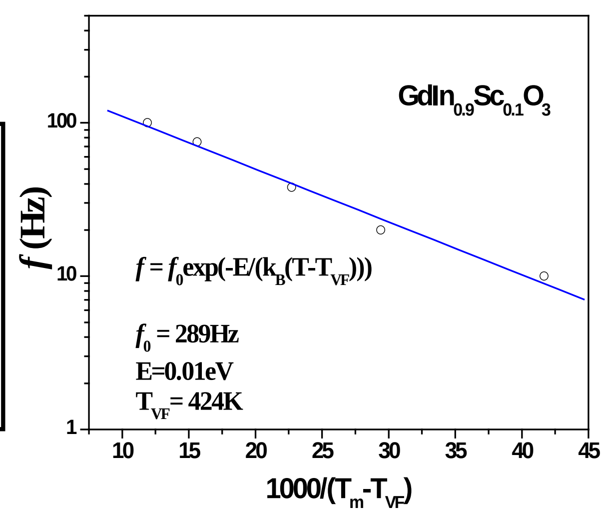

Vogel-Fulcher Plot

- Normal dielectric behavior with high K up to 80 mol% In^{3+}
- $GdInO_3$ shows diffuse phase transition
- $GdSc_{0.1}In_{0.9}O_3$ is a relaxor ferroelectric.

Subtle changes in the BO_5 polyhedra

Trigonal bipyramidal (TBP) structure

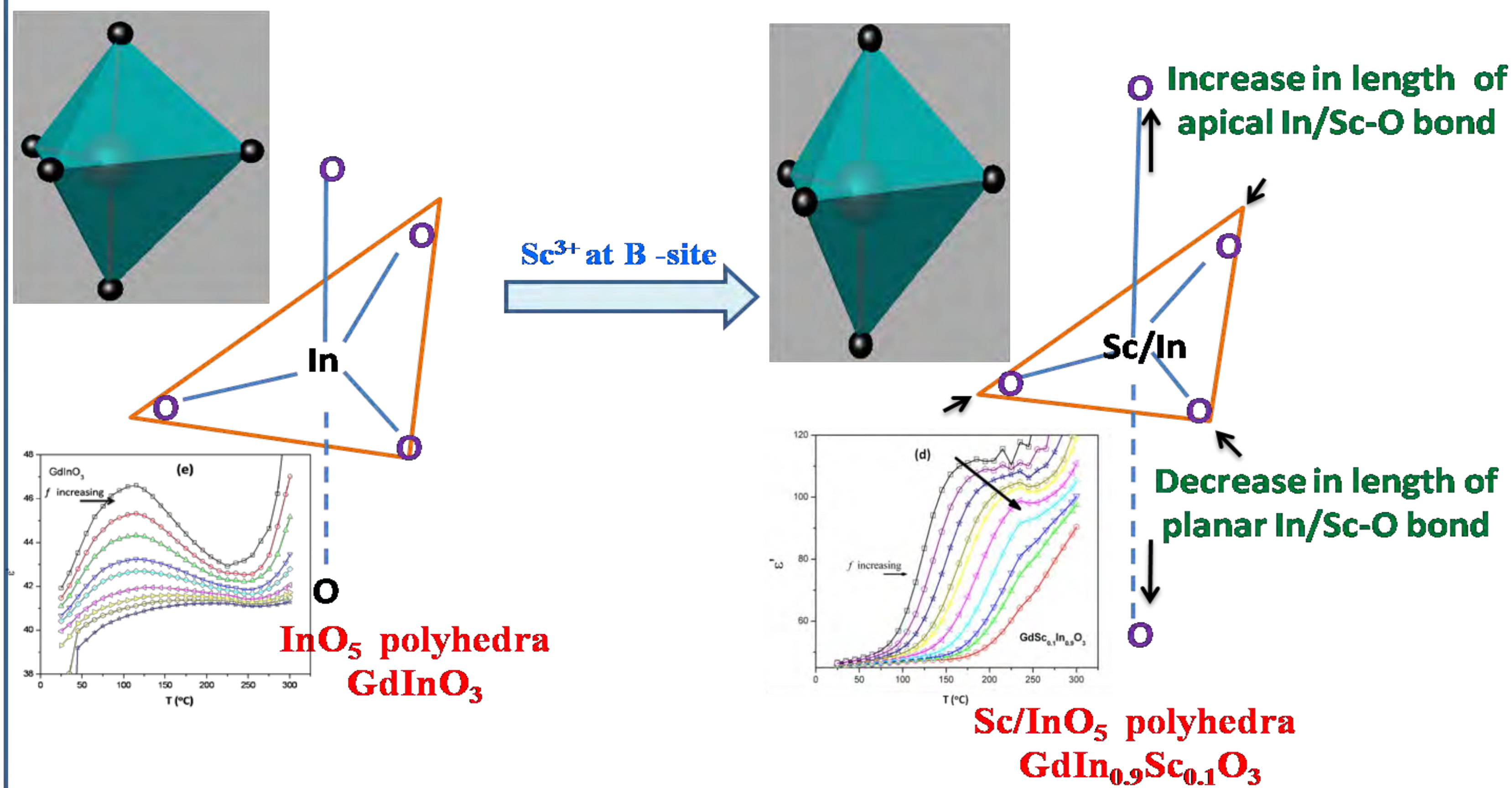

Perhaps the distortion in BO_5 polyhedra is causing difference in electrical properties

Chemistry of Materials 24 (2012) 2186

$YIn_{1-x}Fe_xO_3$ ($0.0 \le x \le 1.0$) system: Potential lead free relaxors

Synthesis: Gel combustion method

Characterization: XRD, Raman & dielectric studies

Hexagonal $YInO_3$

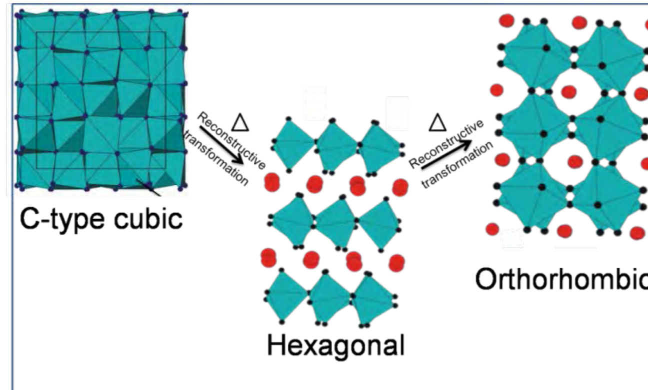

Polymorphs observed for $YIn_{1-x}Fe_xO_3$ system

Fe^{3+} increasing →

Temp	$YInO_3$	10%Fe	20%Fe	30%Fe	40%Fe	50%Fe	60%Fe	70%Fe	80%Fe	90%Fe	$YFeO_3$
(*t*)	0.8295	0.8350	0.8406	0.8463	0.8520	0.8579	0.8638	0.8698	0.8759	0.8820	0.8883
600 °C	C	C	C	C	C	C	C	C	C	C	C
750 °C	C	C	C + Hexa	Hexa	Hexa	Hexa	Hexa	Hexa	Hexa	Hexa	Hexa + Ortho
900 °C	C	Hexa	Hexa	Hexa	Hexa	Hexa	Hexa	Hexa + Ortho	Hexa + Ortho	Hexa + Ortho	Ortho
1150°C	Hexa	Hexa	Hexa	Hexa	Hexa	Hexa + Ortho	Hexa + Ortho	Hexa + Ortho	Hexa + Ortho	Hexa + Ortho	Ortho
1250°C	Hexa	Hexa	Hexa	Hexa	Hexa + Ortho	Hexa + Ortho	Hexa + Ortho	Hexa + Ortho	Hexa + Ortho	Hexa + Ortho	Ortho

Single phasic

Immense bearing of temperature on phase relations

Observation of metastable phases

Raman studies

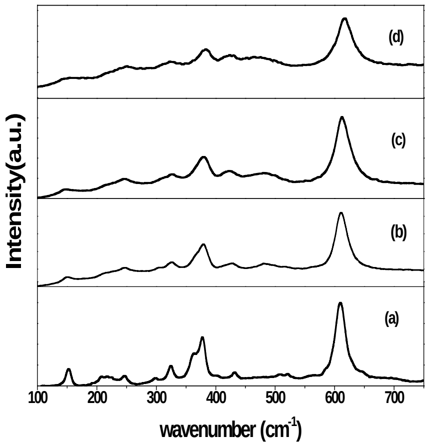

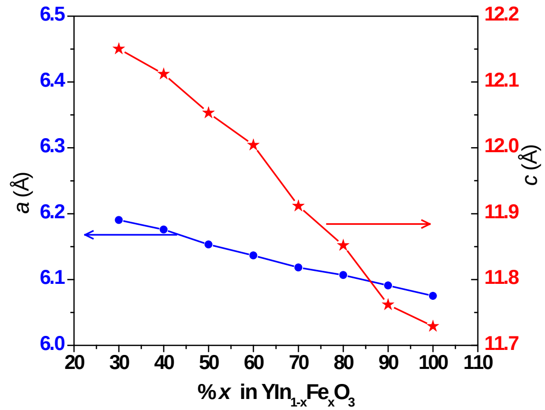

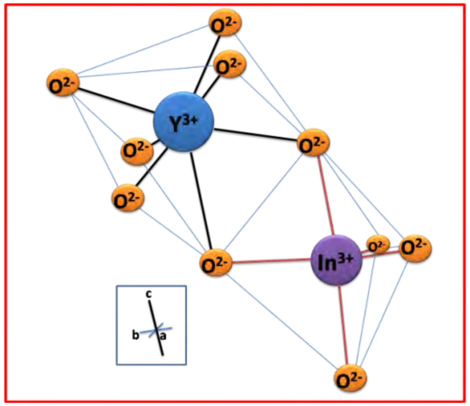

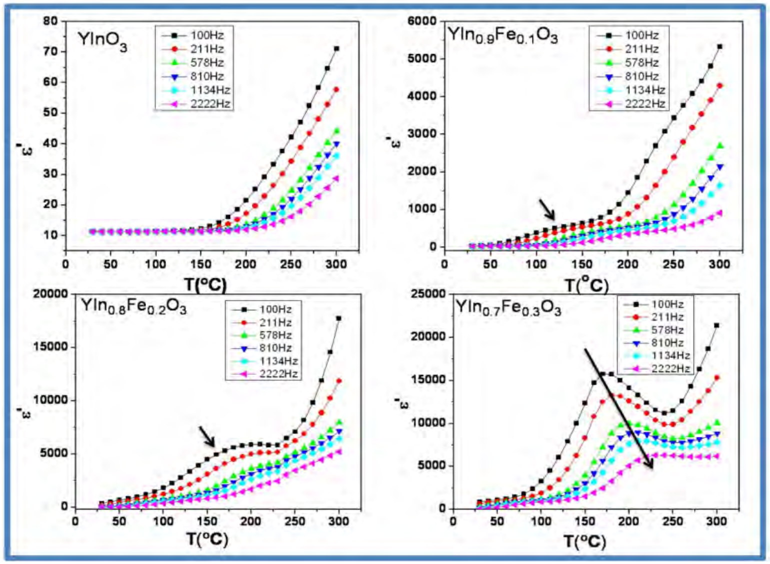

Manifestation in electrical behavior

Highlights: Metastable phases, composition-structural tunability exhibited,

Potential Lead free relaxors

Inorganic Chemistry 53 (2014) 10101

$FeTiTaO_6$: A New Lead-Free Relaxor Ferroelectric

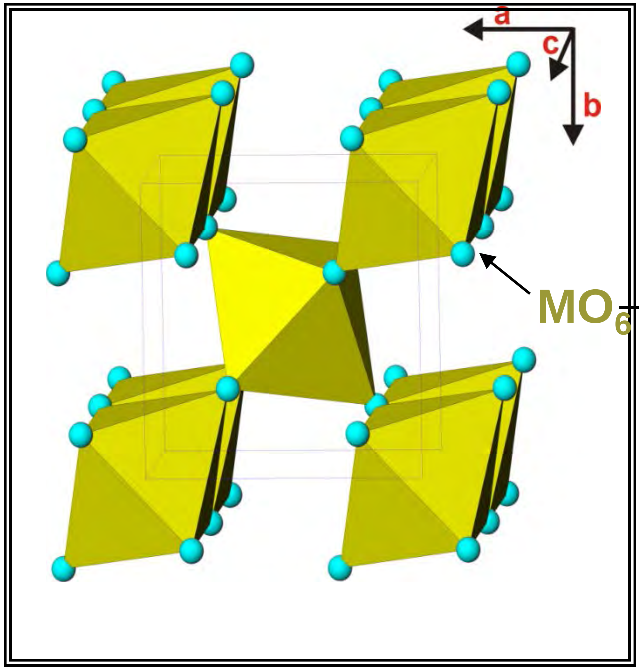

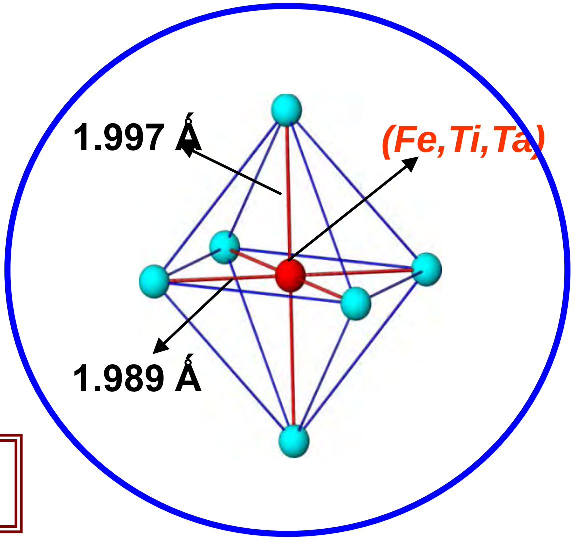

Dielectric data

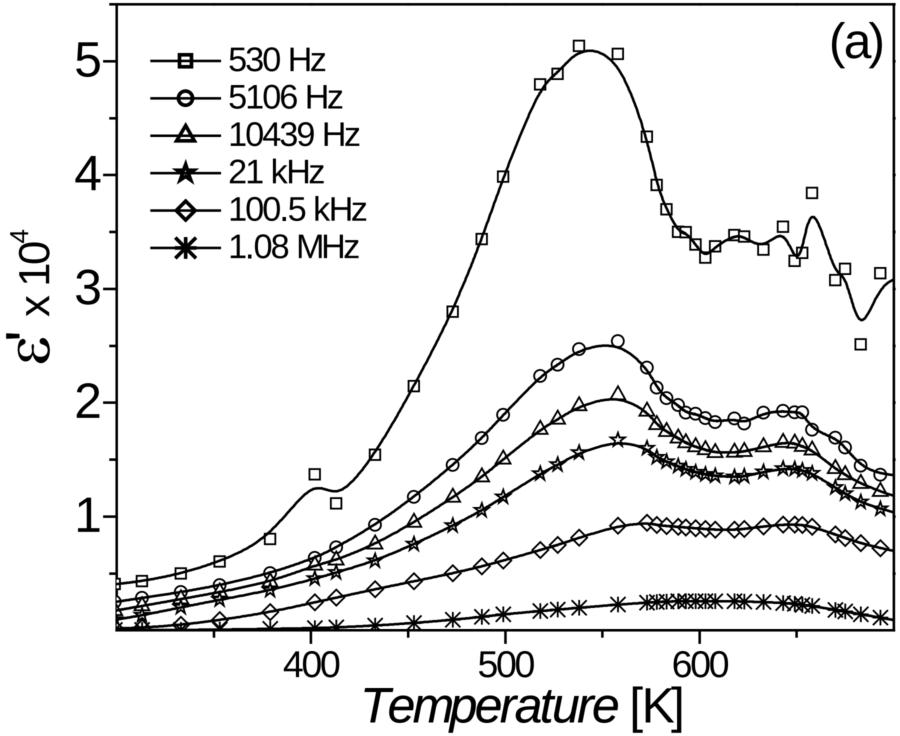

Rutile structure
Space group: $P4_2/mnm$
a = 4.655(4) and c = 3.021(2) Å

Advanced Materials 20 (2008) 1348

Systematic methodology to transform a normal dielectric material to a relaxor based material

$SrTi_{1-2x}Fe_xTa_xO_3$: interplay of composition, structure & cationic disorder

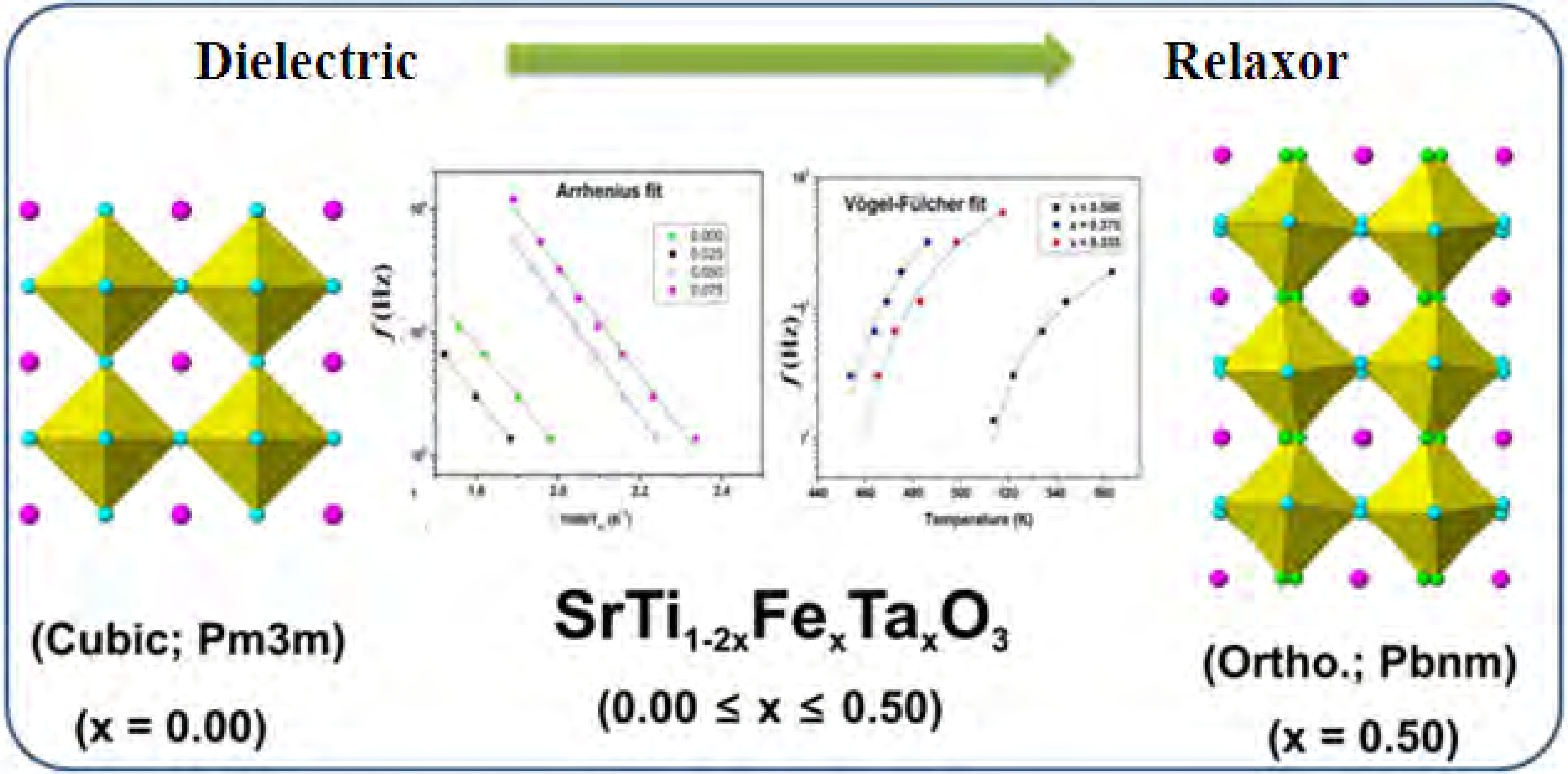

A tunable large dielectric permittivity achieved by optimized cation disorder in orthorhombic structure

Nature Sci. Rep., 6 (2016) 23400

Tailored materials for nuclear applications

$K_2M(PO_4)_2$ ($M = Ce^{4+}, Zr^{4+}$): Inorganic ion exchangers

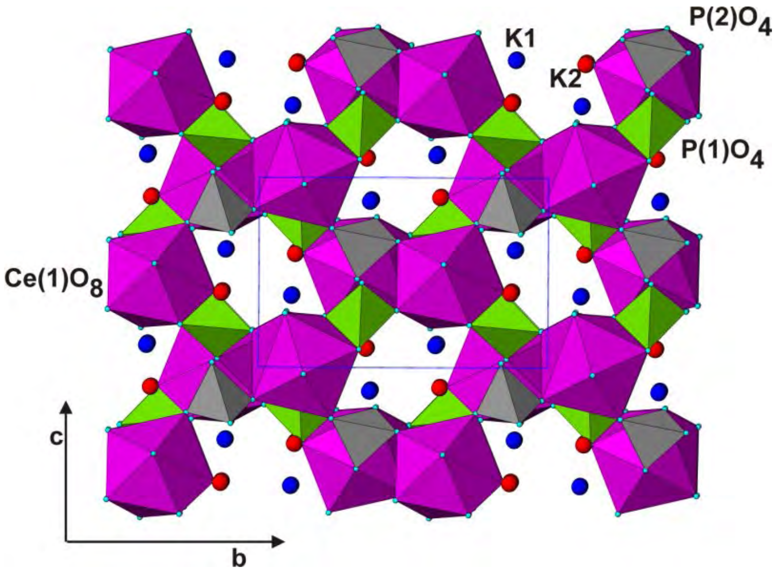

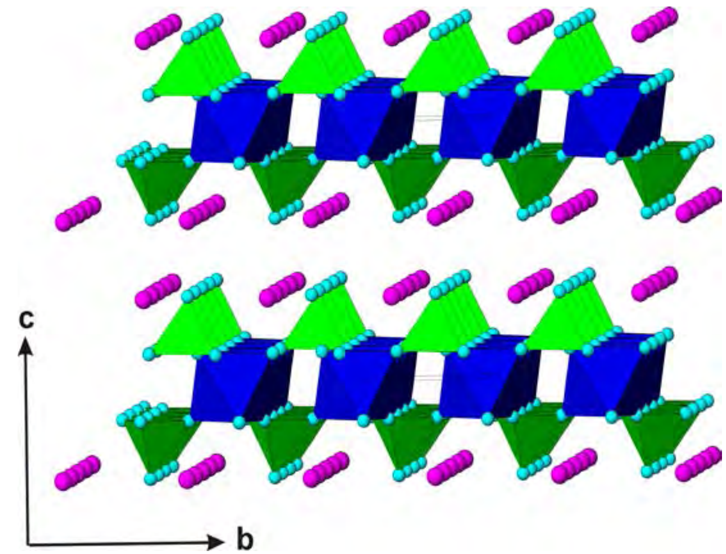

CeO_8 polyhedra linked to two PO_4 groups by sharing edges and corners

3-dimensional anionic frame with composition $[Ce(PO_4)_2]^{2-}$

ZrO_6 octahedra share corners with PO_4 tetrahedra

Two-dimensional sheets with compositions $[Zr(PO_4)_2]^{2-}$ are stacked along the *c*-direction

Monoclinic, $P2_1/n$
a = 9.1020(1) Å, b = 10.8132(1) Å
c = 7.6231(1) Å and β = 111.14(1)°

Rhombohedral, P-3
a = 5.2032(1) Å, c = 9.0538(1) Å

DaltonTrans. 45 (2016) 980 Inorg. Chem., 56 (2017) 3335

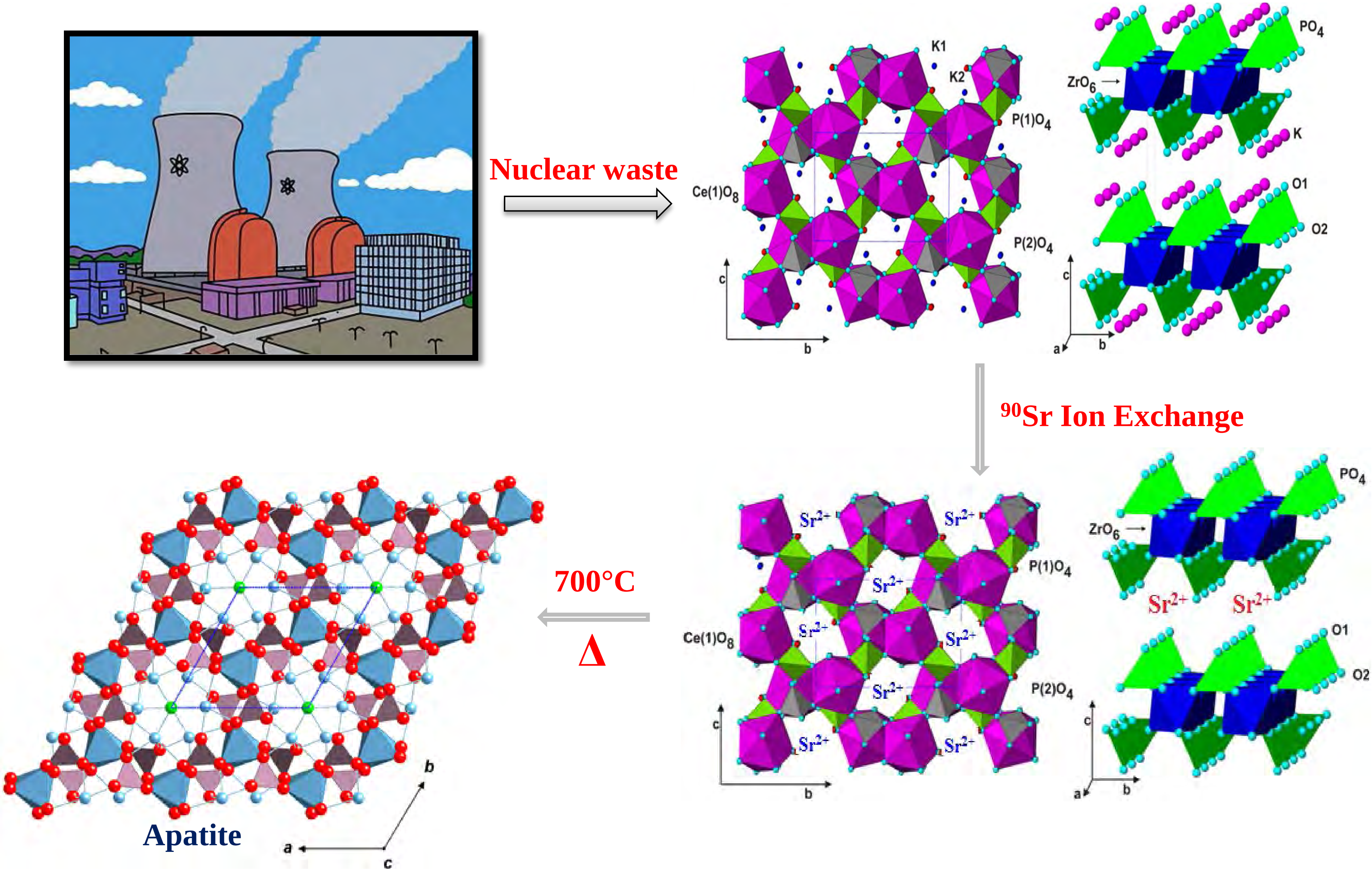

$K_2Ce(PO_4)_2$:Sr and $K_2Zr(PO_4)_2$: Sr converts to apatite type lattice after heat treatment, which are stable matrices for immobilisation of radioactive nuclear waste

General concluding remark

Rational design: Several examples

Structure – property correlation

Disorder, defects and distortion

Soft-chemical methods

Several applications were discussed

Acknowledgements

Indian Academy of Sciences

Colleagues and students:

Rakesh, Farheen, Vinita, Achary, Balaji, Jayakumar, Dimple, Mohsin, Patwe and Samatha

All the collaborators

Thanks for your kind attention

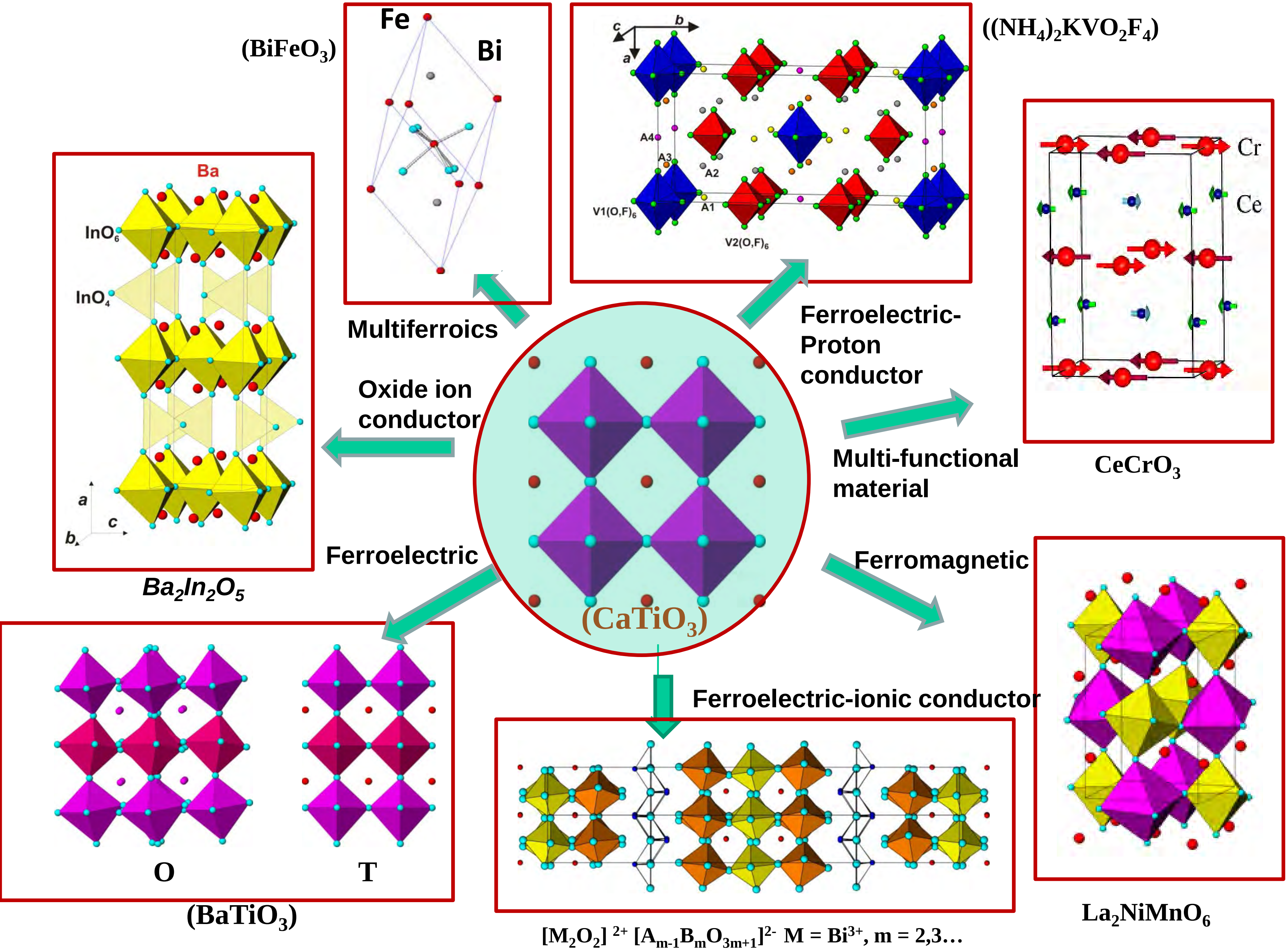

(BiFeO$_3$)
Fe
Bi
Multiferroics
((NH$_4$)$_2$KVO$_2$F$_4$)
A4
A3
A2
A1
V1(O,F)$_6$
V2(O,F)$_6$
Ferroelectric-Proton conductor
Cr
Ce
CeCrO$_3$
Multi-functional material
Ba
InO$_6$
InO$_4$
Oxide ion conductor
Ba$_2$In$_2$O$_5$
Ferroelectric
(CaTiO$_3$)
Ferromagnetic
La$_2$NiMnO$_6$
O
T
(BaTiO$_3$)
Ferroelectric-ionic conductor
$[M_2O_2]^{2+}$ $[A_{m-1}B_mO_{3m+1}]^{2-}$ M = Bi^{3+}, m = 2,3…

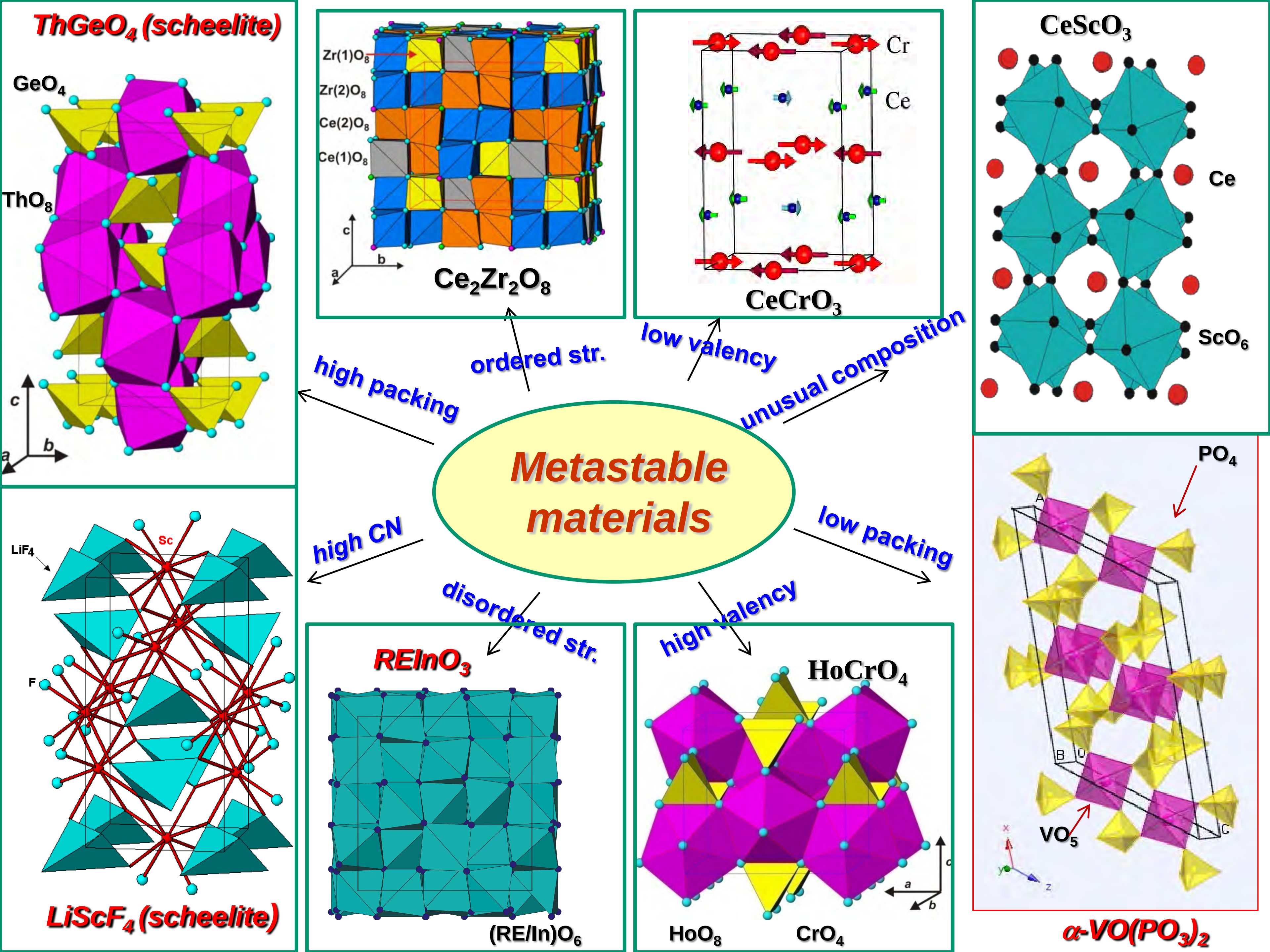

Metastable materials
high packing
ordered str.
low valency
unusual composition
high CN
disordered str.
high valency
low packing
ThGeO4 (scheelite)
GeO4
ThO8
Ce2Zr2O8
Zr(1)O8
Zr(2)O8
Ce(2)O8
Ce(1)O8
CeCrO3
Cr
Ce
CeScO3
Ce
ScO6
α-VO(PO3)2
PO4
VO5
LiScF4 (scheelite)
LiF4
Sc
F
REInO3
(RE/In)O6
HoCrO4
HoO8
CrO4

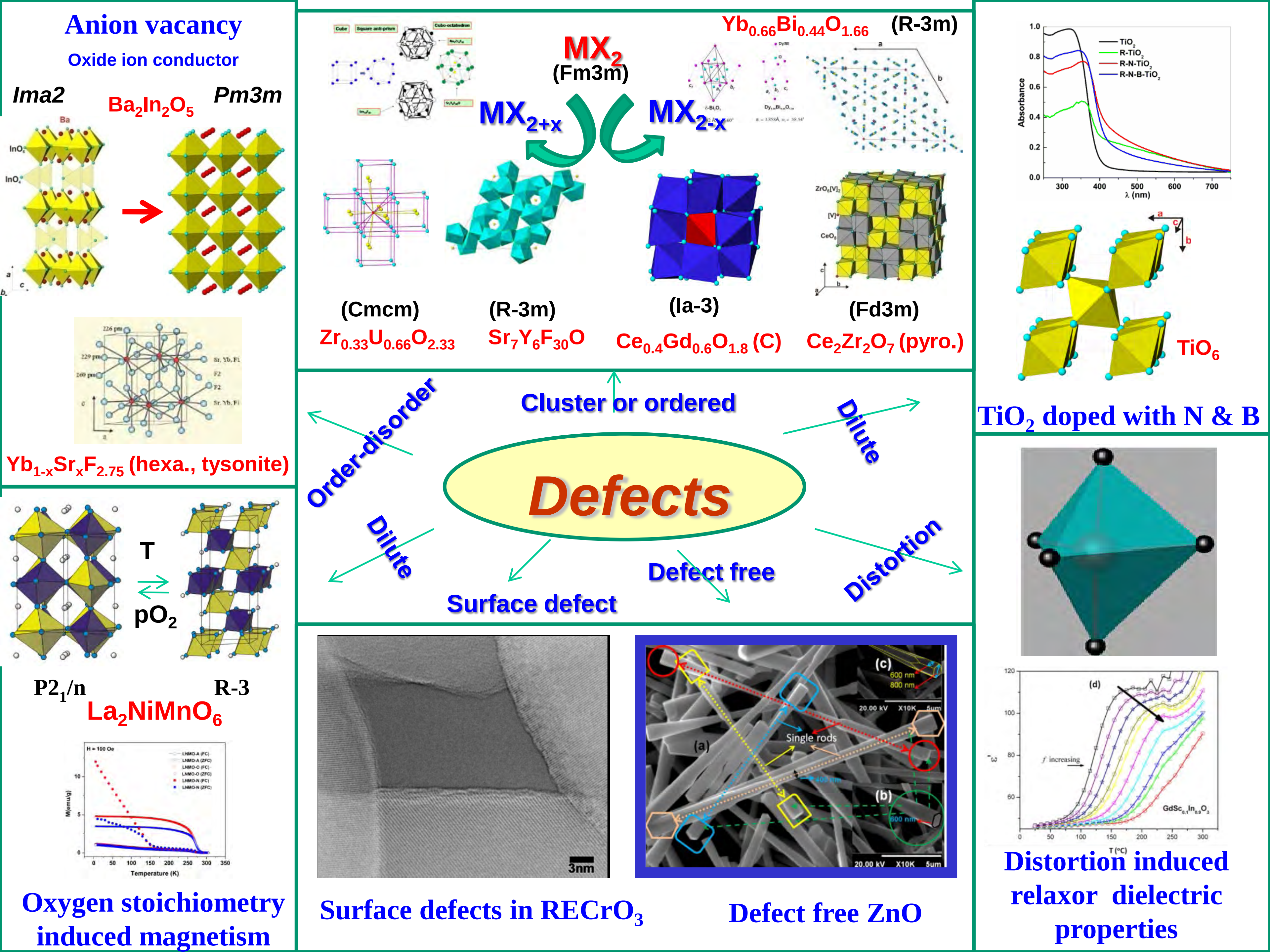

Anion vacancy
Oxide ion conductor
Ima2
$Ba_2In_2O_5$
Pm3m
$Yb_{1-x}Sr_xF_{2.75}$ (hexa., tysonite)
T
pO_2
$P2_1/n$
R-3
La_2NiMnO_6
Oxygen stoichiometry induced magnetism
MX_2
(Fm3m)
MX_{2+x}
MX_{2-x}
$Yb_{0.66}Bi_{0.44}O_{1.66}$
(R-3m)
(Cmcm)
$Zr_{0.33}U_{0.66}O_{2.33}$
(R-3m)
$Sr_7Y_6F_{30}O$
(Ia-3)
$Ce_{0.4}Gd_{0.6}O_{1.8}$ (C)
(Fd3m)
$Ce_2Zr_2O_7$ (pyro.)
Cluster or ordered
Order-disorder
Dilute
Defects
Dilute
Distortion
Surface defect
Defect free
Surface defects in $RECrO_3$
Single rods
Defect free ZnO
TiO_6
TiO_2 doped with N & B
Distortion induced relaxor dielectric properties

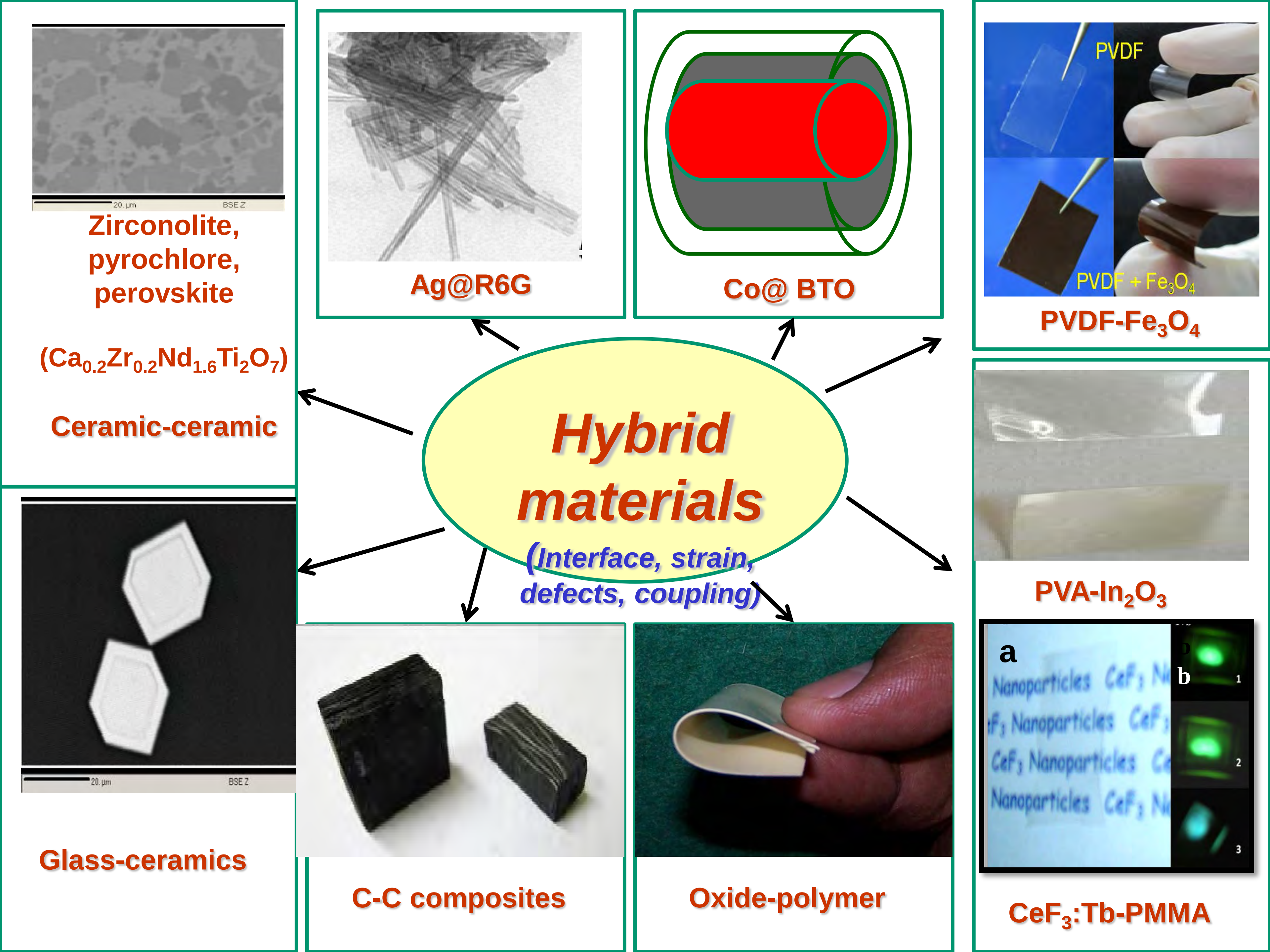
Hybrid materials
(Interface, strain, defects, coupling)
20 μm BSE Z
Zirconolite, pyrochlore, perovskite
($Ca_{0.2}Zr_{0.2}Nd_{1.6}Ti_2O_7$)
Ceramic-ceramic
Ag@R6G
Co@ BTO
PVDF
PVDF + Fe_3O_4
PVDF-Fe_3O_4
PVA-In_2O_3
a
b
1
2
3
CeF_3:Tb-PMMA
20 μm BSE Z
Glass-ceramics
C-C composites
Oxide-polymer